QUANTUM CHROMODYNAMICS AND HADRONS: AN ELEMENTARY INTRODUCTION

Alexander Khodjamirian

Theoretische Physik 1, Fachbereich Physik, Universität Siegen, D-57068, Siegen, Germany

Abstract

Notes of five lectures given at the 2003 European School of High-Energy Physics, Tsakhkadzor, Armenia, September 2003

1. QUARKS AND GLUONS

1.1 Introduction

In Standard Model the properties of quarks and leptons are remarkably similar, as far as the electroweak interactions are concerned. The quarks with six different flavours are grouped into the three doublets (u, d),(c, s),(t, b), in one-to-one correspondence to the three lepton doublets (ν_e, e),(ν_μ, μ), (ν_τ, τ), as shown in the schematic chart in Fig. 1. Quarks and leptons interact in a similar way with the electroweak vector bosons γ, $W^\pm$ and Z. Furthermore, it is anticipated that the universal Higgs mechanism is responsible for the generation of the quark and lepton masses (for more details see [1]).

In addition, quarks interact "on their own", revealing their specific property, the colour charge (*colour*), a conserved quantum number which is absent for leptons. A quark of a given flavour has three different colour states with equal masses and electroweak charges. Colour-induced interactions between quarks are mediated by *gluons*, the massless and electroweakly-neutral spin-1 particles,

In these lectures I will discuss the quark-gluon "corner" of the Standard Model, introducing the basics of Quantum Chromodynamics (QCD), the theory of quark-gluon interactions. Throughout this survey, the main emphasis will be put on the relation between QCD and *hadrons*, the observed bound states of quarks. This first lecture is devoted to the basic properties of the quark-gluon interactions. I will frequently refer to Quantum Electrodynamics (QED), the more familiar theory of electromagnetic (e.m.) interactions, which is a useful prototype of QCD.

In Fig. 2 the Feynman diagram of the electron-muon e.m. scattering is drawn together with the analogous diagram of the quark-quark interaction. For definiteness, I specify the quarks as having d and s flavours, the counterparts of e and μ in the Standard Model. The two interactions have many important similarities:

– the colour-charged quarks emit and absorb gluons in the same way as the electrically charged leptons emit and absorb photons;

– gluon and photon are massless;

– both gluon and photon have spin 1.

Being guided by this analogy, one would expect that gluon exchanges generate a Coulomb-type interquark force, similar to the usual attraction/repulsion between the electrically charged particles. In reality, quark-gluon interactions are far more complicated. In particular, since the colour charge has three components, quarks can change their color states after emitting/absorbing gluons, as indicated on the diagram in Fig. 2. Hence, due to the colour conservation, gluons also carry colour quantum numbers, and, as a result, interact with each other. In fact, it is the gluon self-interaction that makes QCD-dynamics so peculiar. Yet QCD has one basic property in common with QED. Both theories have specific "internal" symmetries, named *local gauge symmetries*, to be discussed below.
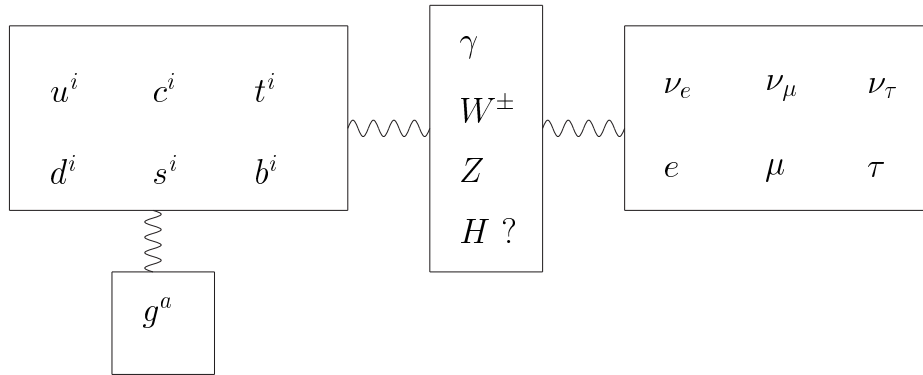
Fig. 1: *Particles of the Standard Model; $i = 1, 2, 3$ and $a = 1, ...8$ are the color indices of quarks and gluons, respectively*
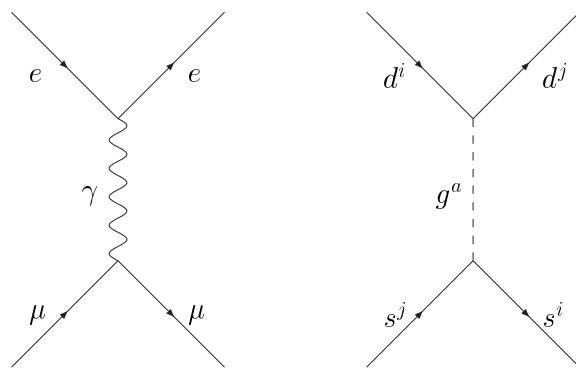

Fig. 2: *Diagrams of lepton-photon (left) and quark-gluon (right) interactions. The dashed line is used to denote gluons and wavy line photon.*

1.2 Local gauge symmetry in QED and QCD

The lepton-photon dynamics is described by one compact formula of the QED Lagrangian,

$$L_{QED}(x) = -\frac{1}{4}F_{\mu\nu}(x)F^{\mu\nu}(x) + \sum_{l=e,\mu,\tau} \bar{\psi}_l(x)(iD_\mu\gamma^\mu - m_l)\psi_l(x), \tag{1}$$

where the physical degrees of freedom of the photon field (the electric and magnetic fields) are combined in the field strength tensor $F_{\mu\nu} = \partial_\mu A_\nu - \partial_\nu A_\mu$, with $\partial_\nu A_\mu \equiv \frac{\partial A_\mu(x)}{\partial x_\nu}$. In the above, $\psi_l(x)$ is the lepton Dirac field with spin 1/2 and mass m_l, and a compact notation for the covariant derivative $D_\mu = \partial_\mu + ieA_\mu$ is introduced. Starting from L_{QED} it is possible to derive Dirac equations for the leptons and Maxwell equations for the photon. Furthermore, Eq. (1) yields the basics elements of the QED Feynman diagrams: the photon and lepton propagators and the lepton-photon interaction vertex. Employing these elements, one obtains the amplitude of a given e.m. process in a form of a perturbative expansion in the numerically small coupling $\alpha_{em} = e^2/4\pi$.

For us the most interesting property of L_{QED} is the gauge symmetry which reveals itself if one locally changes the phase of the lepton fields:

$$\begin{aligned} \psi_l(x) &\rightarrow \psi'_l(x) = exp\left[-i\chi(x)\right]\psi_l(x), \\ \bar{\psi}_l(x) &\rightarrow \bar{\psi}'_l(x) = \bar{\psi}_l(x)exp\left[i\chi(x)\right], \end{aligned} \tag{2}$$

$\chi(x)$ being an arbitrary function of the 4-coordinate x. If one simultaneously adds the derivative of the same function to the photon field:

$$A_\mu \rightarrow A'_\mu(x) = A_\mu(x) + \frac{1}{e}\partial_\mu\chi(x), \tag{3}$$

the Lagrangian (1) remains invariant. It is easy to check that the transformations (2) and (3) leave intact the physical observables, such as the e.m. current $\bar{\psi}_l\gamma_\mu\psi_l$ or $F_{\mu\nu}$. Importantly, the local gauge symmetry implies that the photon mass vanishes, $m_\gamma = 0$. Indeed, adding to L_{QED} a mass term $m_\gamma^2 A_\mu A^\mu$ for the photon field would evidently violate the symmetry because the latter term changes under (3). The particular case $\chi = const$ (when only the lepton fields are transformed) corresponds to the *global* gauge symmetry which is responsible for the e.m. current conservation in QED.

From the mathematical point of view the QED gauge transformations form a *group*. Let me remind that a given set of elements $\{g_i\}$ can be qualified as a group if three conditions are simultaneously fulfilled: 1) a multiplication rule can be defined $g_i * g_k = g_l$, that is, a correspondence is established between a given pair of elements g_i and g_k and a certain third element g_l belonging to the same set; 2) the unit element g_0 exists, so that $g_0 * g_i = g_i$ for each g_i and 3) the inverse element g_k^{-1} can be specified for each g_k, so that $g_k * g_k^{-1} = g_0$. All three conditions are valid for the (infinite and continuous) set of transformations (2) and (3) generated by the set of the arbitrary functions $\chi(x)$. Indeed, performing two gauge transformations one after the other, with $\chi_1(x)$ and $\chi_2(x)$, is equivalent to the gauge transformation with $\chi_{12}(x) = \chi_1(x) + \chi_2(x)$. The unit element of this "multiplication" rule is simply the transformation with $\chi_0(x) \equiv 0$ and the inverse element for each $\chi(x)$ is $-\chi(x)$. Importantly, the group multiplication is commutative (the group is Abelian) because the result of the overlap of two phase transformations is independent of their order. The group we are discussing is called $U(1)$. Mathematically, it is equivalent to the group of rotations of the Cartesian coordinate system around one of its axes. The rotation angle plays the same role as the phase χ.

Gauge transformations in QCD have a more rich geometry. They are somewhat similar to the general rotations in the 3-dimensional space, involving 3×3 matrices, which do not commute. More specifically, a colour gauge transformation of the quark field

$$\psi_q^i(x) = \begin{pmatrix} \psi_q^1(x) \\ \psi_q^2(x) \\ \psi_q^3(x) \end{pmatrix},$$

with a given flavour $q = u, d, s, ...$, involves transitions between different color components, a sort of "rotations of colour coordinates":

$$\psi_q^i(x) \rightarrow \psi_q'^i(x) = U_k^i(x)\psi_q^k(x),$$
$$\bar{\psi}_{q\,i}(x) \rightarrow \bar{\psi}'_{q\,i}(x) = \bar{\psi}_k U_i^{\dagger\,k}(x). \tag{4}$$

The elements of the 3×3 matrix $U_k^i(x)$ depend arbitrarily on the 4-point x. Furthermore, this matrix is unitary:

$$U_k^{\dagger i} U_j^k = \delta_j^k, \tag{5}$$

or, in a symbolic form, $U^\dagger U = 1$. To explain why unitarity is necessary, let me invoke the following physical argument. Since photon does not distinguish quark colours, the only admittable form for the e.m. interaction of quarks is

$$L_{em}(x) = eQ_q \sum_{k=1,2,3} \bar{\psi}_{q\,k}(x)\gamma_\mu \psi_q^k(x)A^\mu(x), \tag{6}$$

where $Q_q = +2/3\,(-1/3)$ for $q = u, c, t\,(d, s, b)$ and the summation goes over the quark colour indices. The gauge transformation (4) applied to the quark fields yields

$$L_{em}(x) \rightarrow L'_{e.m.}(x) = \bar{\psi}_{q\,i}(x)U_k^{\dagger i}(x)\gamma_\mu U(x)_j^k \psi_q^j(x)A^\mu(x). \tag{7}$$

Clearly, only if (5) is valid, L_{em} remains invariant.

The usual exponential representation of the gauge transformation matrix is:

$$U_k^i(x) = \exp\left[-i\sum_{a=1}^{8} \chi^a(x)\frac{(\lambda^a)_k^i}{2}\right]. \tag{8}$$

It contains eight independent and arbitrary functions $\chi^a(x)$ multiplied by eight reference matrices λ^a ($a = 1, ...8$). The latter have the form chosen by Gell-Mann:

$$\lambda^1 = \begin{pmatrix} 0 & 1 & 0 \\ 1 & 0 & 0 \\ 0 & 0 & 0 \end{pmatrix}, \quad \lambda^2 = \begin{pmatrix} 0 & -i & 0 \\ i & 0 & 0 \\ 0 & 0 & 0 \end{pmatrix}, \quad \lambda^3 = \begin{pmatrix} 1 & 0 & 0 \\ 0 & -1 & 0 \\ 0 & 0 & 0 \end{pmatrix},$$

$$\lambda^4 = \begin{pmatrix} 0 & 0 & 1 \\ 0 & 0 & 0 \\ 1 & 0 & 0 \end{pmatrix}, \quad \lambda^5 = \begin{pmatrix} 0 & 0 & -i \\ 0 & 0 & 0 \\ i & 0 & 0 \end{pmatrix},$$

$$\lambda^6 = \begin{pmatrix} 0 & 0 & 0 \\ 0 & 0 & 1 \\ 0 & 1 & 0 \end{pmatrix}, \quad \lambda^7 = \begin{pmatrix} 0 & 0 & 0 \\ 0 & 0 & -i \\ 0 & i & 0 \end{pmatrix}, \quad \lambda^8 = \frac{1}{\sqrt{3}}\begin{pmatrix} 1 & 0 & 0 \\ 0 & 1 & 0 \\ 0 & 0 & -2 \end{pmatrix}. \tag{9}$$

The λ-matrices have the following properties: $\lambda^{a\dagger} = \lambda^a$ (hermiticity), $Tr\lambda^a = 0$, and $[\lambda^a, \lambda^b] = f^{abc}\lambda^c$ (noncommutativity), where f^{abc} are totally antisymmetric constants ($f^{123} = -f^{213}$, etc.). It is easy to check that $U(x)$ defined in (8) obeys unitarity and has a unit determinant $det\,U = 1$. The (infinite and continuous) set of noncommutative U matrices forms a group, which is called $SU(3)$. One may ask: why there are eight independent functions χ^a determining the rotations of the three color states? Isn't eight too many? The point is that the quark fields ψ_q^i are complex functions, hence the matrix $U(x)$ is also a complex function of x determined by 2×9 real functions. Only 8 of them are independent because there are altogether 10 constraints: nine provided by the unitarity relation (5) and one by the unit determinant. With eight "rotation angles" the group $SU(3)$ is of course quite different from the group of rotations in three dimensions which has only 3 parameters.

1.3 QCD Lagrangian

The QCD Lagrangian has to be exactly symmetric with respect to the local gauge transformations (4) with matrices (8). This property serves as a guiding principle for constructing L_{QCD}.

We start from the part of the Lagrangian which describes the propagation of free quarks:

$$L_{quark}(x) = \sum_{q=u,d,s,...} \left(\sum_{k=1,2,3} \bar{\psi}_{q\,k}(x)(i\partial_\mu \gamma^\mu - m_q)\psi_q^k(x) \right), \qquad (10)$$

and yields the usual Dirac equation for spin 1/2 particle for each quark with a given flavour and colour. Similar to the case of QED, the expression (10) is not invariant with respect to the local gauge transformations (4). An additional term with derivatives of $\chi^a(x)$ remains:

$$L_{quark}(x) \rightarrow L_{quark}(x) + \sum_{q=u,d,s,...} \bar{\psi}_{q\,i}(x) \left[iU_k^{\dagger\,i}(x)\partial_\mu U_j^k(x) \right] \gamma^\mu \psi_q^j(x). \qquad (11)$$

To restore gauge invariance one follows the same scenario as in QED or in the electroweak theory [1]. The idea (put forward long ago by Yang and Mills) is to introduce "compensating" spin-1 fields interacting with quark fields. There should be one separate spin-1 field for each of the eight degrees of freedom determining the gauge transformations (4). In this way eight gluons enter the game, with the following quark-gluon interaction term added to the Lagrangian:

$$L_{int}(x) = g_s \sum_{q=u,d,s,...} \bar{\psi}_{q\,i}(x)\frac{(\lambda^a)_k^i}{2}\gamma^\mu \psi_q^k(x) A_\mu^a(x). \qquad (12)$$

Here g_s is the dimensionless coupling analogous to e in L_{QED}. In contrast to e.m. interaction, where the photon field is electrically neutral, the gluon fields also carry colour charge, so that the colour state of a quark changes after emitting/absorbing a gluon. The colour of the gluon distinguished by the index $a = 1...8$ can be identified with a superposition of quark and antiquark colours. For example the gluon field $A_\mu^1(x)$ is in the same colour state as the quark-antiquark pair $\bar{\psi}_{q\,1}\psi_q^2 + \bar{\psi}_{q\,2}\psi_q^1$. The A_μ^a-fields in (12) have to be gauge-transformed in the following way:

$$\frac{\lambda^a}{2}A_\mu^a(x) \rightarrow U(x)\frac{\lambda^a}{2}A_\mu^a(x)U^\dagger(x) - \frac{i}{g_s}\partial_\mu U(x)U^\dagger(x), \qquad (13)$$

so that the overall change of L_{int} cancels the symmetry breaking term on r.h.s. of (11). It is a simple exercise to check that the combination of transformations (4) and (13) leaves the sum $L_{quark} + L_{int}$ invariant. We see that in QCD the "compensating" transformation of gluon fields (13) is more complicated than its analog (3) in QED: the addition of the derivative over χ-functions is accompanied by a "color rotation".

To complete the Lagrangian one has to add a gauge-invariant term describing the propagation of gluon fields :

$$L_{glue}(x) = -\frac{1}{4}G_{\mu\nu}^a(x)G^{a\,\mu\nu}(x), \qquad (14)$$

where

$$G_{\mu\nu}^a = \partial_\mu A_\nu^a - \partial_\nu A_\mu^a + g_s f^{abc} A_\mu^b A_\nu^c, \qquad (15)$$

is the gluon field-strength tensor. The local gauge invariance of L_{glue} implies that gluons are massless. At the same time, $G_{\mu\nu}^a$ is a more complicated object than its QED analog $F_{\mu\nu}$. Indeed, substituting (15) to (14), we notice that not only the terms quadratic in A_μ^a emerge (propagation of gluons) but also the three- and four-gluon vertices (gluon self-interactions). Note that formally, both properties of

Quark propagator	$\langle 0|T\{\psi_q^i(x)\bar{\psi}_{qk}(0)\}|0\rangle = i\delta_k^i \int d^4p \left(\frac{p_\alpha \gamma^\alpha + m_q}{p^2 - m_q^2}\right) e^{-ipx}$
Gluon propagator	$\langle 0|T\{A_\mu^a(x)A_\nu^b(0)\}|0\rangle = -i\delta^{ab} \int d^4k \frac{g_{\mu\nu}}{k^2} e^{ikx}$
Quark-gluon vertex	$g_s \bar{\psi}_q(x)\gamma_\mu \frac{\lambda^a}{2}\psi_q(x)A^{a\,\mu}(x)$
3-gluon vertex	$-\frac{g_s}{2}f^{abc}[\partial_\mu A_\nu^a(x) - \partial_\nu A_\mu^a(x)]A^{b\mu}(x)A^{c\nu}(x)$
4-gluon vertex	$-\frac{g_s^2}{4}f^{abc}f_{ade}A_\mu^b(x)A_\nu^c(x)A^{d\mu}(x)A^{e\nu}(x)$

Table 1: *Propagators and vertices in QCD.*

gluons: colour quantum number and self-interactions are due to the noncommutativity of the gauge-transformation group (the fact that $f_{abc} \neq 0$). The final form of QCD Lagrangian is obtained by adding together the three pieces introduced above:

$$L_{QCD} = L_{glue} + L_{quark} + L_{int}$$
$$= -\frac{1}{4}G_{\mu\nu}^a G^{a\mu\nu} + \sum_q \bar{\psi}_q(iD_\mu\gamma^\mu - m_q)\psi_q\,, \qquad (16)$$

where $D_\mu = \partial_\mu - ig_s\frac{\lambda^a}{2}A_\mu^a$. To summarize, L_{QCD} describes not only quark-gluon interactions but also *gluodynamics*, the specific gluon self-interactions which have no analog in QED [1].

The quark and gluon propagators and vertices derived from L_{QCD} are collected in Table 1. The formula of the gluon propagator has a certain degree of freedom related to the fact that the physical massless gluon has only two polarization/spin states whereas the field A_μ^a has four components. To make things working, one follows the same recipe as in QED. An additional constraint on the gluon field is introduced, the so called gauge-fixing condition. The gluon propagator given in Table 1 corresponds to the usual Feynman gauge. Note that in QCD purely gluonic loop diagrams are possible, in which case one has to take care of subtracting the contributions of unphysical components of A_μ^a also in these loops. It is usually done by adding specially designed fictitious particles (the so called Fadeev-Popov ghosts) which only appear in the loops, and are not shown in Table 1.

Feynman diagrams in QCD are obtained employing the quark-gluon propagators and vertices as building blocks. However, the use of diagrams makes sense only if the perturbative expansion in g_s is meaningful. To obey this condition, the *quark-gluon coupling*

$$\alpha_s = \frac{g_s^2}{4\pi}\,, \qquad (17)$$

---

[1]In QCD "light emits light" at the level of the fundamental interactions entering Lagrangian, as opposed to QED where light-by-light interaction appears only as $O(\alpha_{em}^2)$ quantum correction (when photons exchange virtual electrons via box diagrams). For a classical Maxwellian electrodynamics, self-interacting e.m. fields would mean "new physics beyond standard theory". I am not aware of any discussions of photon self-interactions in the times before quantum field theory. Interestingly, the light emitting light was mentioned in poetry. I found the following sentence written in XIII century by Armenian poet Kostandin Erznkazi [2]: "And so the light was born from the light, the great light of Sun..." (in translation from Armenian)
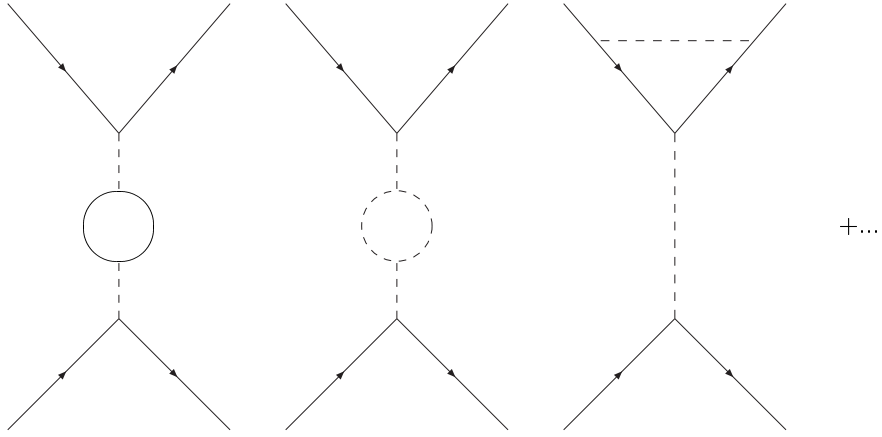
Fig. 3: *Some of the diagrams corresponding to quantum loop corrections to the quark-quark scattering*

the QCD analog of the e.m. coupling $\alpha_{em} = e^2/4\pi$, has to be sufficiently small, $\alpha_s \ll 1$. If this condition is fulfilled, then, for example, the $O(\alpha_s)$ diagram of the quark-quark interaction in Fig. 2 dominates over the higher-order diagrams with additional gluon exchanges. One has then a tractable situation, with quarks and gluons propagating quasi-freely. Thus, there is an important question to be addressed: how large is α_s ?

1.4 Running of the quark-gluon coupling

To answer the above question, one has to investigate quantum effects in QCD, i.e., creation and annihilation of virtual gluons and quarks described by loop diagrams. In QED, which we use as a prototype, quantum loops generate very small effects, such as Lamb shift (the correction to the Coulomb force due to the virtual electron-positron pairs) or the $O(\alpha_{em})$ one-loop correction to the muon magnetic moment. These effects, being accessible in precision experiments, play a minor role in the bulk of electromagnetic processes.

In QCD, quark-gluon loops are far more pronounced and play a crucial role in determining α_s. To have a closer look, let us consider the quark-quark scattering amplitude. In the lowest-order (at the tree level) the amplitude is given by the one-gluon exchange diagram shown in Fig. 2 for the particular choice of quark flavours. Having at hand the Feynman rules in QCD it is easy to write down the amplitude:

$$\mathcal{A} = \frac{4\pi\alpha_s}{q^2} \left(\bar{\psi}_{s\,i} \gamma_\mu \frac{(\lambda^a)^i_k}{2} \psi^k_s \right) \left(\bar{\psi}_{d\,j} \gamma^\mu \frac{(\lambda^a)^j_l}{2} \psi^l_d \right) , \tag{18}$$

where $q^2 < 0$ is the momentum transfer squared. Below I will also use the notation for the momentum scale: $Q \equiv \sqrt{Q^2}$, where $Q^2 = -q^2 > 0$. Considering $O(\alpha_s)$ corrections to the amplitude (18) one encounters diagrams shown in Fig. 3. They contain gluon or quark loops inserted within the exchanged gluon line or in the vertices. These loop effects turn out to be extremely important for evaluating α_s.

Let me first explain the loop diagram calculation in more detail. After substituting propagators of virtual particles, one arrives at four-dimensional Feynman integrals over the 4-momentum k flowing

inside the loop, typically:

$$I_{loop}(q, m_q) = \int \frac{d^4k}{(2\pi)^4} \frac{...}{(k^2 - m_q^2)((k + q)^2 - m_q^2)} \,, \tag{19}$$

where the explicit expression in the numerator (depending on the spin of the loop particles) does not play role in our discussion. For simplicity, I will also put to zero the quark masses, a reasonable approximation if $Q \gg m_q$. To calculate loop integrals, one usually employs the method of dimensional regularization. The idea is to lower the number of dimensions in the integral (19) making it convergent. One replaces 4 by a generic integer number D, then calculates the integral as a function of D and after that considers the result at an arbitrary noninteger $D = 4 - \epsilon$, schematically:

$$I_{loop}(q, 0) = \int d^4k f(k, q) \rightarrow \mu^{(4-D)} \int d^D k f(k, q) = I(q, \mu, D) \rightarrow I(q, \mu, 4 - \epsilon) \,. \tag{20}$$

The auxiliary mass scale μ is introduced to keep unchanged the physical dimension of the integral. The major advantage of dimensional regularization is in preserving gauge symmetry of the amplitudes at each step of the calculation. The divergent part of the integral in this scheme is represented in a form of terms proportional to $1/\epsilon$. A generic expression for the loop integral has a form:

$$I_{loop}(q, 0) \rightarrow \mu^{4-D} \int \frac{d^D k}{(2\pi)^D} \frac{...}{k^2(k + q)^2} = I_1 \log(-q^2/\mu^2) + \frac{1}{\epsilon} + I_2 \,. \tag{21}$$

where $I_{1,2}$ are calculable finite coefficients.

QCD is a *renormalizable* theory (similar to QED), which means one can absorb all divergent $1/\epsilon$ terms into the so called Z -factors. Multiplying by Z_g^{-1} the coupling g_s, and by the corresponding factors the quark masses, quark and gluon fields, one defines the finite (renormalized) quantities; e.g., the renormalized coupling is $g_s^{ren} = Z_g^{-1} g_s$. Having in mind the validity of the renormalization procedure I will simply ignore divergent terms appearing in (21) and in other loop integrals.

Adding the $O(\alpha_s)$ diagrams in Fig. 3 to the tree-level amplitude, results in the same expression (18), but with α_s replaced by an *effective coupling* depending on the momentum scale:

$$\alpha_s^{eff}(Q) \equiv \alpha_s \left[1 - \frac{\alpha_s}{4\pi} \left(\beta_0 \log \frac{Q^2}{\mu^2} + const \right) \right] \,, \tag{22}$$

where a shorthand notation

$$\beta_0 = 11 - \frac{2}{3} n_f \tag{23}$$

is introduced. Here n_f is the number of "active" quark flavours in the loop diagrams. Only those quarks which have $m_q \ll Q$ contribute to $\alpha_s^{eff}(Q^2)$. Importantly, β_0 is positive, because the term 11 originating from the gluon loops exceeds the quark-loop contribution $2n_f/3$ (since $n_f < 6$ in any case).

Taking α_s^{eff} at a different scale Q_0,

$$\alpha_s^{eff}(Q_0) \equiv \alpha_s \left[1 - \frac{\alpha_s}{4\pi} \left(\beta_0 \log \frac{Q_0^2}{\mu^2} + const \right) \right] \,, \tag{24}$$

and dividing (22) by (24) one obtains, with an accuracy of $O(\alpha_s^2)$:

$$\alpha_s^{eff}(Q) = \alpha_s^{eff}(Q_0) \left[1 - \frac{\alpha_s^{eff}(Q_0)}{4\pi} \beta_0 \log \frac{Q^2}{Q_0^2} \right] \,, \tag{25}$$

the relation between effective couplings at two different scales. The approximation (25) is valid only if $\alpha_s^{eff}(Q_0)$ is sufficiently small and the higher-order corrections are negligible. Remarkably, (25) predicts
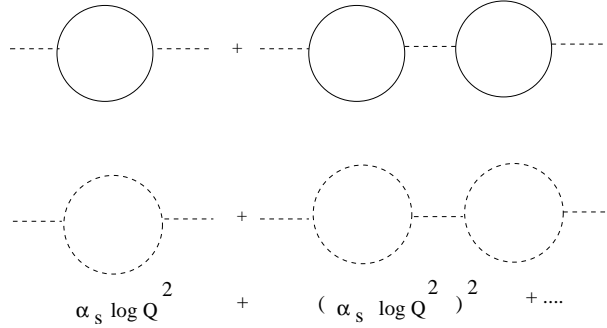
Fig. 4: *One- and two-loop diagrams contributing to the running of α_s.*

that $\alpha_s^{eff}(Q)$ decreases when the momentum scale Q increases. Thus, if the perturbative expansion in α_s is applicable at certain Q_0, it should behave even better at $Q > Q_0$.

Note that (25) still has to be improved. At $Q \to \infty$ the logarithm becomes very large driving the combination $\alpha_s \log Q^2$ to rather big values, so that the $O\left([\alpha_s log\left(Q^2/Q_0^2\right]^2\right)$ correction originating from the two-loop diagrams shown in Fig. 4 becomes important, and the whole perturbative construction is again in danger. Fortunately, a systematic resummation of all $O\left([\alpha_s log\left(Q^2/Q_0^2\right]^n\right)$ corrections is possible. In practice, one does not need to calculate all multiloop diagrams, which would be a tremendous work. Instead, the renormalization-group method is used, which is however beyond our scope. The resulting expression for the *running coupling* is:

$$\alpha_s(Q) = \frac{\alpha_s(Q_0)}{1 + \frac{\alpha_s(Q_0)}{4\pi}\beta_0 \cdot \log\frac{Q^2}{Q_0^2}} \, . \tag{26}$$

(hereafter the superscript 'eff' is omitted). Expanding the denominator in (26) and retaining only the first two terms we return to the relation (25).

1.5 Asymptotic freedom

A consistent use of the running QCD coupling is possible if one can find a range of Q where $\alpha_s(Q)$ is numerically small. The first indications that α_s is indeed small at large momentum transfers were obtained in the studies of deep-inelastic lepton-nucleon scattering (to be discussed in Lecture 3). This remarkable discovery paved the way for using QCD perturbation theory with the running coupling in many other processes.

To trace the numerical behavior of $\alpha_s(Q)$ one has to fix the coupling at a certain large scale using an experimental input. One possibility is the decay of Z-boson to a quark-antiquark pair. Quarks originating in this decay inevitably build hadrons in the final state (see the next subsection). To avoid hadronic complexity, one measures the total inclusive width $\Gamma(Z \to hadrons)$, so that the probabilities of all possible quarks $\to$ hadrons transitions add up to a unit. The majority of $Z \to hadrons$ events observed at LEP has a spectacular structure of two hadronic jets originating from the initial, very energetic quark and antiquark ($E_q = E_{\bar q} = m_Z/2$ in the Z rest-frame), see, e.g. [3]. On the other hand, the share of ≥ 3-jet events in $Z \to hadrons$, with additional jets originating from gluons and/or from secondary quark-antiquark pairs, is small. This observation clearly indicates that the quark-gluon coupling at the scale m_Z is small, or in other words the initial quark pair interacts weakly during the short time after its creation.

The perturbative diagrams of $Z \to q\bar q$ ($q = u, d, s, c, b$) including the gluon emission $Z \to \bar qqG$ are shown in Fig. 5. Evaluating these diagrams one gets the perturbative expansion for the total hadronic
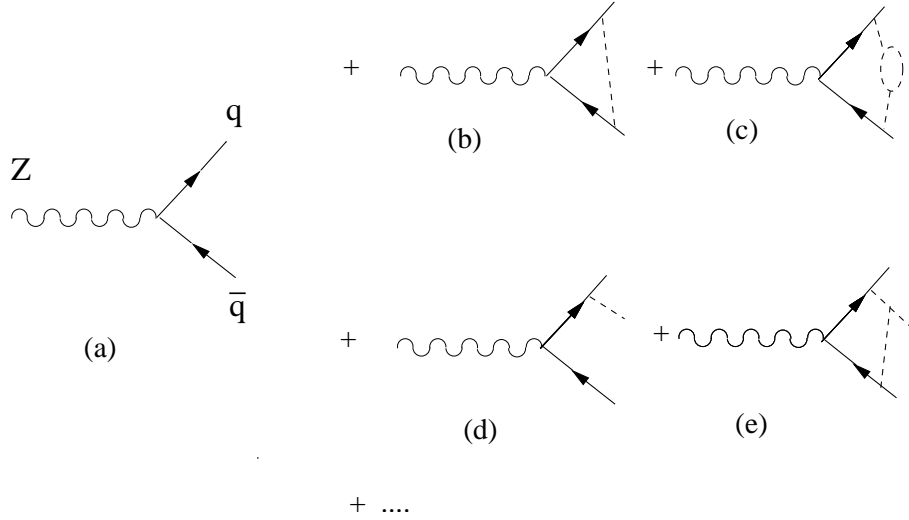
Fig. 5: *The lowest-order diagram (a) and some of the higher-order in α_s diagrams (b-d) determining the total width $Z \rightarrow$ hadrons.*

width, schematically:

$$\Gamma(Z \rightarrow hadrons) = \sum_{q=u,d,s,..} \left[\Gamma(Z \rightarrow \bar{q}q) \left(1 + C_1^q \alpha_s(m_Z) + C_2^q \alpha_s^2(m_Z) + ... \right) \right.$$
$$\left. + \Gamma(Z \rightarrow \bar{q}qG) \left(1 + C_1^{qG} \alpha_s(m_Z) + ... \right) + ... \right], \qquad (27)$$

where $\Gamma(Z \rightarrow \bar{q}q)$ and $\Gamma(Z \rightarrow \bar{q}qG)$ (the latter starting from $O(\alpha_s)$) are the corresponding perturbative widths, and $C_{1,2}^q, C_1^{qG},..$ are the calculable coefficients. Smallness of α_s allows to neglect all higher-order corrections starting, say from $O(\alpha_s^3)$. In the above expression α_s is taken at the scale m_Z, the characteristic scale in this process. One can trace how the running coupling builds up in (27), by summing up all logarithmic corrections generated by the loop insertions similar to the one shown in Fig. 4c.

Comparing the result (27) of the theoretical calculation with the experimental data yields [4]:

$$\alpha_s(m_Z) \simeq 0.12. \qquad (28)$$

As expected, it is a rather small number, so that the whole perturbative treatment turns out to be quite consistent. Using (26) and (28), one predicts $\alpha_s(Q)$ at lower scales. The curve plotted in Fig. 6 is taken from [4] and reflects the current status of the running coupling, including all known (and reasonably small) higher-order corrections to (26). As can be seen in this figure, there is a wide region spreading up to $Q \sim 1$ GeV, where α_s is small and perturbative QCD is applicable. Furthermore, α_s extracted from various processes at different scales agrees with the running behavior predicted in QCD. The most spectacular consequence of (26) is the vanishing of the running quark-gluon coupling at $Q \rightarrow \infty$, revealing that QCD is asymptotically free.

1.6 Confinement and hadrons

Quite an opposite situation takes place in the quark-gluon interactions at small momentum transfers (at long distances). According to (26), if one starts from $Q \gg 1$ GeV and drifts towards smaller scales, α_s grows to $O(1)$ at $Q < 1$ GeV (see Fig. 7). Perturbation theory becomes useless in this region, because e.g. in the quark-quark scattering, an infinite amount of higher-order quark-gluon diagrams has to be
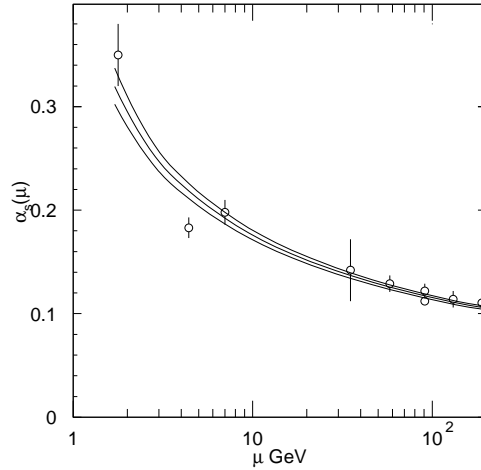
Fig. 6: *The dependence of $\alpha_s(\mu)$ on the running scale μ [4]: the upper and lower curves indicate the theoretical uncertainty, the points with errors are the values of α_s extracted at different scales using various methods.*

taken into account. Moreover, at a certain momentum scale denoted by Λ_{QCD} the denominator in (26) vanishes and $\alpha_s(Q)$ diverges. The relation between $\alpha_s(Q)$ and Λ_{QCD} following from (26) is:

$$\alpha_s(Q) = \frac{2\pi}{\beta_0 \log\left(\frac{Q}{\Lambda_{QCD}}\right)} \, . \tag{29}$$

The experimentally measured value (28) corresponds, roughly, to

$$\Lambda_{QCD} = 200 - 300 \text{ MeV}. \tag{30}$$

I skip some details concerning the dependence of Λ_{QCD} on the number of active quark flavours, and on the theoretical scheme of the loop-diagram evaluation, relevant for the higher-order corrections to (29). The important fact is that (29) and (30) were derived neglecting the quark masses. We could have put to zero the quark masses in L_{QCD} from the very beginning, starting with a theory without dimensionful parameters. The emergence of an intrinsic energy scale in a theory with dimensionless coupling g_s (*dimensional transmutation*) is a specific property of QCD, due entirely to quantum effects.

The breakdown of perturbation theory and the exploding behavior of $\alpha_s(Q)$ at $Q \to \Lambda_{QCD}$ are actually anticipated. Long before QCD was invented it was known that at long distances quarks and antiquarks strongly interact and form *hadrons*, the quark-antiquark (*meson*) and 3-quark (*baryon*) bound states. The properties of hadrons will be considered in a more systematic way in the next Lecture. For the present discussion it is important that the characteristic energy scale of hadronic interactions is of $O(\Lambda_{QCD})$. Hence, it is quite natural that the formation of hadrons is due to the strong, nonperturbative quark-gluon force emerging in QCD at momenta $\sim \Lambda_{QCD}$.

Moreover, hadronic matter is the only observable form of quarks and gluons at long distances. In any process of quark and antiquark production, independent of the energy/momenta involved, quarks form hadrons in the final state [2]. Note that in QED the situation is quite different: isolated leptons and other electrically charged particles are observed, and the e.m. bound states (e.g., hydrogen atom, positronium or muonium) can always be split into constituents if a sufficient energy is supplied.

---

[2]There is one exception: t-quark, decaying via weak interactions, is too short-lived to be bound by quark-gluon forces.
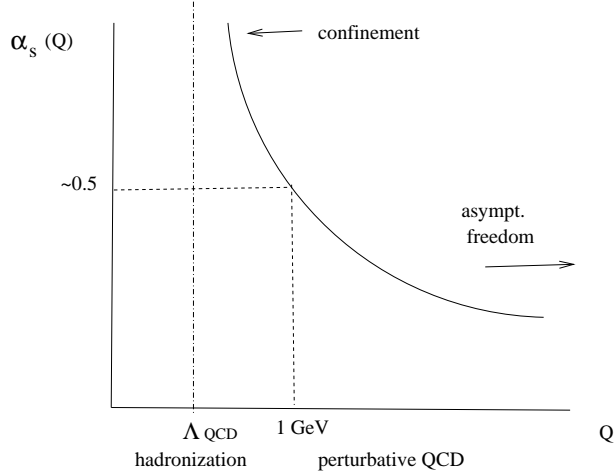
Fig. 7: *Schematic view of the α_s behavior at different scales.*

In QCD, the non-observation of free colour-charged particles (quarks, antiquarks and gluons) is arranged in a form of the *colour confinement* principle, postulating that all observable states, i.e., all hadrons, have to be colour-neutral. The confinement principle was never rigorously proved, because of our limited ability to work with QCD beyond perturbation theory. Nevertheless, all experimental results concerning hadrons, as well as lattice simulations of QCD at long distances, unambiguously support colour confinement.

Before the era of QCD the search for free quarks was very popular among experimentalists. The fractional electric charge was a smoking-gun signal to be observed. The hunt for quarks was a part of many accelerator experiments. Not surprisingly, free quarks have never been found at accelerators or in other places (in cosmic rays, water, ice, meteorites etc.). Nowadays, one would hardly invest efforts in the search for free quarks. We are confident that QCD obeys confinement.

1.7 Quark masses

The current intervals of quark masses presented in the Particle Data Tables [4] are:

$$m_u = 1.5 \div 4.5 \text{ MeV}, \quad m_c = 1.0 \div 1.4 \text{ GeV}, \quad m_t = 174.3 \pm 5.1 \text{ GeV};$$
$$m_d = 5 \div 8.5 \text{ MeV}, \quad m_s = 80 \div 155 \text{ MeV}, \quad m_b = 4.0 \div 4.5 \text{ GeV}. \tag{31}$$

The fact that the masses are spread over five orders of magnitude, is a reflection of some fundamental flavour physics not related to QCD, e.g. the Higgs mechanism of the Standard Model. Hence, the masses m_q entering QCD Lagrangian (16) are "external" parameters. At the same time quark masses are evidently changed in the presence of quark-gluon interactions. At long distances, within hadrons, each quark acquires, roughly speaking, an extra addition of $O(\Lambda_{QCD})$ to its "bare" mass. It is however very difficult, if not impossible at all, to define this *constituent* quark mass in a model-independent way. Representing the hadron mass as a sum of the constituent quark masses plus some interaction energy, e.g. for a meson:

$$M_{meson} = m_q^{constit} + m_{\bar{q}}^{constit} + E_{int}, \tag{32}$$

one can always redistribute the part of E_{int} between the quark and antiquark masses. Since free, on-shell quarks are not observed, the usual definition of the particle mass (the minimal possible energy of the one-particle state) does not work.

The mass values presented in (31) have nevertheless quite a definite meaning. These are "short-distance" masses of the virtual quarks. As we already know, at large virtualities quark propagation is

(a)   (b)

Fig. 8: *The free quark propagator (a) and the gluon correction to it (b).*

quasi-free and a consistent use of perturbation theory derived from QCD Lagranigian is possible. In particular, the free quark propagator

$$S(p) = \frac{p_\alpha \gamma^\alpha + m_q}{p^2 - m_q^2} \tag{33}$$

is applicable at $|p^2| \gg \Lambda_{QCD}^2, m_q^2$, with the bare mass m_q from L_{QCD}. Furthermore, at short distances the quark-gluon interactions are calculable in terms of series in α_s. The quark propagating at short distances can emit and absorb a gluon (see diagram (b) in Fig. 8). From the experience with the running coupling one expects such loops to be important. Adding the loop diagram to the free propagator yields the same expression as (33) with m_q replaced by an effective mass depending on the momentum scale

$$m_q^{eff}(Q) = m_q \left[1 - \frac{\alpha_s}{4\pi} \left(\gamma_0 \log \frac{Q^2}{\mu^2} + const \right) \right], \tag{34}$$

where I omit the divergent part, knowing that it will be absorbed by renormalization. In this case the scale $Q \sim \sqrt{|p^2|}$ is determined by the virtuality of the quark and $\gamma_0 = 4$ is the result of the explicit calculation. Again, as in the case of α_s, we can relate the effective masses at two different scales. Writing down the above equation for another scale Q_0 and using instead of m_q^{eff} a conventional notation $\overline{m}_q$ we obtain:

$$\overline{m}_q(Q) = \overline{m}_q(Q_0) \left(1 - \left(\frac{\gamma_0}{\beta_0} \right) \frac{\alpha_s(Q_0)}{4\pi} \beta_0 \log \frac{Q^2}{Q_0^2} \right), \tag{35}$$

where I have multiplied and divided the logarithmic term by β_0 and used $\alpha_s = \alpha_s(Q_0)$ which is correct with $O(\alpha_s)$ accuracy. With the same accuracy the expression in parentheses can be transformed further:

$$1 - \left(\frac{\gamma_0}{\beta_0} \right) \frac{\alpha_s(Q_0)}{4\pi} \beta_0 \log \frac{Q^2}{Q_0^2} \simeq \left(1 - \frac{\alpha_s(Q_0)}{4\pi} \beta_0 \log \frac{Q^2}{Q_0^2} \right)^{\gamma_0/\beta_0}. \tag{36}$$

Using (25) we obtain

$$\bar{m}_q(Q) = \bar{m}_q(Q_0) \left(\frac{\alpha_s(Q)}{\alpha_s(Q_0)} \right)^{\gamma_0/\beta_0}, \tag{37}$$

the formula for the *running mass*. A more rigorous derivation is possible using the renormalization group method. Also in recent years, the higher-order corrections to (37) have been calculated.

The masses presented in [4] are the running masses (also called $\overline{MS}$ masses if one specifies the particular renormalization procedure) normalized at some large scale. The light u, d, s quark masses are traditionally taken at $Q = 2$ GeV, whereas a more appropriate scale for the heavy c and b quark masses is the quark mass itself, $Q = m_c$ and $Q = m_b$, respectively, (which means, e.g., the virtuality of the c quark is $p^2 = -m_c^2$). The fact that quark masses run with the scale, is in accordance with the absence of isolated quarks among observable states.

1.8   Two branches of QCD

To summarize, QCD yields two qualitatively different pictures of quark-gluon interactions:

1) at high momentum-transfers i.e., at short average distances, perturbative expansions in α_s are applicable in terms of Feynman diagrams with quark and gluon propagators and vertices. In this region the scale-dependence (running) of the coupling and quark masses should be properly taken into account.

2) at low scales, that is, at long distances, one loses control over perturbative interactions between individual quarks and gluons; the latter strongly interact and form hadrons.

Accordingly, QCD is being developed in two different directions. The first one deals with short-distance physics accessible at high energies. One studies specific processes/observables calculable (at least partly) in a form of a perturbative expansion in α_s. A typical short-distance process is the jet production in Z decays considered above, other examples will be presented in Lecture 3.

The second direction deals with nonperturbative quark-gluon interactions at long distances and with hadron dynamics. A complete analytical evaluation of hadronic masses and other parameters directly from L_{QCD} is not yet accessible. Instead, a powerful numerical method of simulating QCD on the space-time lattice has been developed. Lattice QCD has become a separate field, which is beyond the scope of these lectures (for a pedagogical introduction see e.g.,[5]). Still there is a lot of interesting advances in the long-distance 'branch'' of QCD, so that I will only be able to cover a part of them. As demonstrated in Lecture 2, many important features of hadron spectroscopy follow from QCD at the qualitative level. The relation of long-distance dynamics to the nontrivial structure of the QCD vacuum will be discussed in Lecture 4. An approximate analytical method of QCD sum rules based on this relation and used to calculate hadronic parameters will be overviewed in Lecture 5.

One might think that physics of hadrons plays a secondary role, because the most important direct tests of QCD in terms of quarks and gluons are done at short distances. Let me emphasize the fundamental importance of hadron dynamics by mentioning two topical problems:

1) *The origin of the nucleon mass*

Proton and neutron are the lowest and most stable baryons, with the quark content uud and udd, respectively. Their masses

$$m_p \simeq m_n \simeq 940 \,\text{MeV}\,, \tag{38}$$

are substantially larger than the tripled quark mass $m_{u,d} = O(\text{few MeV})$. We conclude that $\sim 99\%$ of the baryon matter in the Universe is not related to the "fundamental" quark masses generated by the Higgs mechanism or from some other flavour dynamics. The bulk of the baryon mass is due to the long-distance quark-gluon interactions. Indeed, adding a "constituent" mass of $O(\Lambda_{QCD})$ to each quark, one gets the order-of-magnitude value of $m_{p,n}$. Certainly, the problem of the nucleon mass is quite fundamental and has to be solved within long-distance QCD.

2) *Extracting electroweak parameters from B decays*

The weak decays of B mesons (the bound states of b quark and light antiquark) represent a valuable source of information on fundamental aspects of electroweak interactions, such as the quark-mixing CKM matrix and the origin of CP-violation (see [6]). One topical example is the $B \to \pi l \nu_l$ decay observed at B factories [4]. This decay (see Fig. 9) is driven by the $b \to u$ weak transition, proportional to V_{ub}, one of the poorly known CKM matrix elements. In order to extract this fundamental parameter from the experimentally measured partial width, one needs to divide out the hadronic $B \to \pi$ transition amplitude (form factor). The latter is essentially determined by the long-distance quark-gluon interactions.

Below, in Lecture 5 we will discuss the (approximate) solutions of the two abovementioned problems.
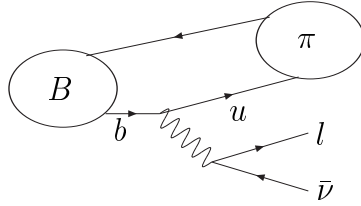
Fig. 9: $B \rightarrow \pi l \nu_l$ *decay involves a hadronic transition between B and π states.*

2. FROM QUARKS TO HADRONS

2.1 Mesons and baryons

Let us now have a closer look at the properties of hadrons [3], the bound states of quarks. There are lots of experimental data on hadrons accumulated in the Review of Particle Physics [4]. As we shall see, employing various symmetries of QCD, it is possible to predict, at least qualitatively, many observable regularities of hadronic spectra and interactions.

The pre-QCD quark model of hadrons failed to explain why only mesons ($\bar{q}q$), baryons (qqq) and antibaryons ($\bar{q}\bar{q}\bar{q}$) are observed. Why, for example, the diquark (qq) or four-quark ($qqqq$) bound states are absent? In QCD, one immediately gets an explanation based on the colour confinement principle. The quark-antiquark and three-quark combinations can form colour-singlet states, whereas diquark and four-quark compounds are always colour-charged. The colour-singlet meson state is obtained by simply summing over the colour indices of the quark and antiquark. For example, the π^+-meson has the following flavour/colour structure:

$$|\pi^+\rangle = \frac{1}{\sqrt{3}} \sum_{i=1}^{3} |u^i \bar{d}_i\rangle . \tag{39}$$

The way baryons are built is less trivial. Two quarks are arranged in a coloured *diquark* state $\epsilon_{ijk}|q^j q^k\rangle$, where ϵ_{ijk} is totally antisymmetric with $\epsilon_{123} = 1$. This state has the colour SU(3)-transformation properties of an antiquark (with a colour index i). Hence, we can obtain a colour-neutral state combining diquark with the third quark and summing over colours in the same way as in mesons. One important example of a three-quark baryon state [4] is Ω^- baryon with spin 3/2:

$$|\Omega\rangle = \frac{1}{\sqrt{6}} \sum_{i,j,k=1}^{3} \epsilon_{ijk}|s^i s^j s^k\rangle. \tag{40}$$

With respect to the flavour and spin, this state is totally symmetric: all quark have the same flavour and parallel spins. Therefore, colour degrees of freedom provide the antisymmetry demanded by the Pauli principle for any bound state of fermions.

---

[3]The word 'hadron' was coined by Okun in [7] where he wrote: "It is reasonable to call strongly interacting particles hadrons, and the corresponding decays - hadronic. In Greek the word hadros means "large","massive", in contrast to the word "leptos", which means "small","light". The term hadron refers to long-lived mesons and baryons, as well as to resonances."

[4]Note that if there were four colours of quarks, with the corresponding SU(4) symmetry, baryons would have been built from four quarks, with profound consequences for the physical world, e.g., atoms with fractional electric charge.

2.2 Quark model of hadrons

The hadron decompositions (39) and (40) resemble chemical formulae, displaying the content of a composite state. In reality hadrons are far more complicated than atoms and molecules, because the masses of the u, d, s quarks are smaller than the QCD long-distance scale: $m_{u,d} \ll \Lambda_{QCD}$ and $m_s < \Lambda_{QCD}$. Hence, light quarks are purely relativistic and the number of quarks, antiquarks and gluons within a hadron cannot be fixed. Since QCD is a quantum field theory, additional quark-antiquark pairs or gluons are created and annihilated inside the bound states *virtually*, i.e. within the time/distance intervals of $O(1/\Lambda_{QCD})$. As a result, the general decomposition of the physical pion state is not simply (39) but rather

$$| \pi^+ \rangle = \ | u^i \bar{d}_i \rangle + \sum_{q=u,d,s,..} | u^i \bar{d}_i q^j \bar{q}_j \rangle + | u^k (\lambda^a)^i_k \bar{d}_i G^a \rangle + ... , \qquad (41)$$

where G denotes a gluon, the Lorentz indices are not specified and a summation over colour indices is implied. In the above sum, the first term represents a state with the minimal particle content (the so called valence-quark content), and ellipses indicate all other multiparticle fluctuations. Naturally, all components of the pion state have to be colourless, with the same $u\bar{d}$ overall flavour, to obey the colour-neutrality and flavour conservation. We conclude that hadrons are, in general, many-body systems with relativistic constituents. Therefore, simple quantum-mechanical models with an interquark potential cannot fully describe pion or other light-quark hadrons.

Before attempting to solve the QCD dynamics, it is useful to apply the symmetries of QCD Lagrangian. The space-time (Lorentz-Poincare) invariance implies that the total angular momentum (or total spin) J of a hadron is a well defined and conserved quantum number. In addition P- and C- parities are conserved in QCD (as opposed to the electroweak theory). Therefore, for a given hadron, the spin-parity combination J^P (J^{PC} for flavour-neutral hadrons) is the next important signature after the mass. Spin-parities are indicated for each observed hadron in its entry in [4].

To proceed in hadron spectroscopy, let us have a more detailed look at the mesons having the same flavour content $u\bar{d}$ as π^+. Each meson state is a complicated coherent decomposition similar to (41). Nevertheless, since J^P is conserved, it is sufficient to consider the valence-quark component to count all possible combinations of J^P starting from the lowest possible spin. The total angular momentum of the valence quark-antiquark state is a sum of the quark and antiquark spins plus the orbital angular momentum:

$$\vec{J} = \vec{S} + \vec{L} , \qquad (42)$$

where $\vec{S} = \vec{s}_q + \vec{s}_{\bar{q}}$ is the total quark spin; $S = 1(0)$ if the individual spins are parallel (antiparallel). Accordingly, there are two possible states with $L = 0$ and $J = S$. One is with $J^P = 0^-$ (pion) and the other with $J^P = 1^-$ (ρ meson). The negative P-parity attributed to these states is obtained from the following rule: $P = -(-1)^L$. Notice an additional minus which has to be added to account for the so called "intrinsic" P-parity of the relativistic quark-antiquark system. Turning to the states with $L = 1$, one encounters three mesons with $S = 1$ ($J^P = 0^+, 1^+, 2^+$) and one with $S = 0$ ($J^P = 1^+$). They are listed in Table 2 according to the classification of [4]. A similar counting can be done for $L = 2, 3, ...$, predicting $J > 2$ mesons. Some of them can be found in [4]. Generally, it is rather difficult to observe hadrons with higher spins. Having larger masses, these states have many decay channels and, therefore, a large total width, complicating their experimental identification in a form of a resonance. Baryons from u, d, s quarks with different J^P listed in [4] can also be interpreted, at least qualitatively, in terms of three-quark valence states with the orbital momentum L between diquark and the third quark.

The angular momentum is not the only source of excited hadron resonances. There are mesons which have the same J^P as π or ρ but a larger mass. These states are somewhat similar to the radially excited levels in a potential. For the pion a natural candidate of such excitation is the $\pi'(1300)$ state with $J^P = 0^-$, whereas ρ meson has at least two experimentally established radially-excited partners with $J^P = 1^-$: $\rho'(1450)$ and $\rho''(1700)$ [4]. Note that because the orbital momentum L is not conserved in relativistic theory, the $L = 2$ state with $J^P = 1^-$ cannot be simply distinguished from the "radial

	S=0		S=1	
L	J^P	meson	J^P	meson
0	0^-	$\pi(140)$	1^-	$\rho(770)$
1	1^+	$b_1(1235)$	0^+	$a_0(980)$
			1^+	$a_1(1260)$
			2^+	$a_2(1320)$

Table 2: *Spectrum of the lowest $u\bar{d}$ states.*

excitation" of the $L = 0$ state with the same spin-parity, - another difficulty for the potential models of light-quark hadrons. Ultimately, one has to think in terms of purely relativistic extended objects, some kind of *quark-gluon strings* having a spectrum of "radial" and J excitations. However, attempts to derive a string picture for hadrons directly from L_{QCD} were not successful so far.

Quark-gluon interaction is flavour-independent. Therefore, given that a $u\bar{d}$ meson with a certain J^P exists, the mesons with the same J^P containing all possible quark-antiquark flavour combinations should also be observed. The flavour partners of the pion (ρ-meson) with $J^P = 0^-$ ($J^P = 1^-$) are listed in Table 3. Almost all of them have been observed; the masses and other characteristics are given in [4]. The only temporary exceptions are the pseudoscalar $b\bar{b}$ meson (η_b) and the vector $\bar{b}c$ meson (B_c^*). These two states are not yet in [4], due mainly to experimental reasons.

The *heavy quarkonia*, i.e., the mesons consisting of heavy quark and antiquark ($\bar{c}c$ or $\bar{b}b$) are of a special interest. Here the masses of interacting quarks are large enough compared to their characteristic energies within hadrons: $m_{b,c} \gg \Lambda_{QCD}$. In other words, heavy quarks are nonrelativistic objects with respect to QCD interactions. It is therefore possible to approximate the quark-gluon interactions with a nonrelativistic potential, putting the hadronic calculus on the safe ground of quantum mechanics. The Coulomb quark-antiquark potential $V(r) = \alpha_s/r$, derived from the one-gluon exchange, is valid at small distances. To provide quark confinement, a certain long-distance part of the potential, infinitely growing at $r \to \infty$ should also exist (e.g., oscillator or linear potential). This part of the potential cannot be directly calculated from L_{QCD} and is usually modeled and fitted to the observed quarkonium spectra. Importantly, numerical studies of QCD on the lattice confirm the existence of the confining potential force between heavy quark and antiquark.

2.3 Isospin

In addition to the exact colour- and space-time symmetries, QCD Lagrangian possesses approximate flavour symmetries originating from the pattern of quark masses. Since the latter are generated by some external mechanism, the flavour symmetries do not have fundamental roots in QCD. Nevertheless, they provide very important relations for hadron masses and hadronic amplitudes.

Let us start with the u and d quarks and rewrite the QCD Lagrangian, isolating these two flavours:

$$L_{QCD} = \bar{\psi}_u(iD_\mu\gamma^\mu - m_u)\psi_u + \bar{\psi}_d(iD_\mu\gamma^\mu - m_d)\psi_d + L_{glue} + L_{s,c,b,t}. \qquad (43)$$

The smallness of the u and d masses, $m_u \sim m_d \ll \Lambda_{QCD}$, implies that also their difference is small:

$$m_d - m_u \ll \Lambda_{QCD}. \qquad (44)$$

	u	d	s	c	b
$\bar{u}$	π^0, η, η'	π^-	K^-	D^0	$\bar{B}^-$
	ρ^0, ω	ρ^-	K^{*-}	D^{*0}	$\bar{B}^{*-}$
$\bar{d}$	π^+	π^0, η, η'	$\bar{K}^0$	D^+	$\bar{B}^0$
	ρ^+	ρ^0, ω	$\bar{K}^{*0}$	D^{*+}	$\bar{B}^{*0}$
$\bar{s}$	K^+	K^0	η, η'	D_s	$\bar{B}_s$
	K^{*+}	$\bar{K}^{*0}$	ϕ	D_s^*	$\bar{B}_s^*$
$\bar{c}$	$\bar{D}^0$	D^-	$\bar{D}_s$	η_c	$\bar{B}_c$
	$\bar{D}^{*0}$	D^{*-}	$\bar{D}_s^*$	J/ψ	$\bar{B}_c^*$
$\bar{b}$	B^+	B^0	B_s	B_c	η_b
	B^{*+}	B^{*0}	B_s^*	B_c^*	Υ

Table 3: *Pseudoscalar ($J^P = 0^-$) (upper lines) and vector ($J^P = 0^-$) (lower lines) mesons with different flavour content.*

Neglecting this difference we use a new notation for the common u, d quark mass:

$$m_u \simeq m_d \simeq \tilde{m}. \tag{45}$$

In this approximation,

$$L_{QCD} \simeq L_{QCD}^{(u=d)} = \overline{\Psi}(D_\mu \gamma^\mu - \tilde{m})\Psi + L_{glue} + .., \tag{46}$$

where a new, two-component spinor field (doublet) is introduced:

$$\Psi = \begin{pmatrix} \psi_u \\ \psi_d \end{pmatrix}, \quad \overline{\Psi} = (\bar{\psi}_u, \bar{\psi}_d).$$

The theory described by the r.h.s. of (46) is not exactly QCD, but is very close to it. The new Lagrangian $L_{QCD}^{(u=d)}$ contains two degenerate quark flavours and has a symmetry with respect to the general phase rotations in the "two-flavour space":

$$\Psi \to \Psi' = \exp\left(-i \sum_{a=1}^{3} \omega^a \frac{\sigma^a}{2}\right)\Psi, \quad \overline{\Psi} \to \overline{\Psi}' = \overline{\Psi} \exp\left(i \sum_{a=1}^{3} \omega^a \frac{\sigma^a}{2}\right), \tag{47}$$

where ω^a are arbitrary (x-independent) parameters and $\sigma^1, \sigma^2, \sigma^3$ are the 2×2 Pauli matrices. The symmetry transformations (47) form a group SU(2) [5].

[5]The number of independent parameters for SU(2) is determined in the same way as we did for SU(3) in Lecture 1: one counts the number of independent elements in the unitary 2×2 matrix with the unit determinant.

One has to emphasize that the approximate SU(2)-flavour symmetry emerges "by chance", simply because the u and d quark masses turn out to be almost degenerate. Note also that e.m. interaction violates this symmetry, due to different electric charges of u and d quarks. But this $O(\alpha_{em})$ effect is again small, at the same level of $\sim 1\%$, as the $O(\frac{m_d - m_u}{\Lambda_{QCD}})$ violation due to the quark mass difference.

The approximate degeneracy of u and d flavours manifests itself in hadrons. Replacing u quarks by d quarks or vice versa in a given hadron, yields a different hadron which has a very close mass and other properties. This qualitative prediction is nicely confirmed by the measured mass differences between proton (uud) and neutron (udd), $\pi^+ (\bar{u}d)$ and $\pi^0 ([\bar{u}u - \bar{d}d]/\sqrt{2})$, $K^+ (u\bar{s})$ and $K^0 (d\bar{s})$, etc.. The typical mass splittings for the $u \leftrightarrow d$ hadronic partners are at the level of few MeV. Thus, QCD nicely explains the origin of *isospin* symmetry introduced by Heisenberg in 30's in nuclear physics, to describe the similarities between the "mirror" isotopes, obtained from each other by interchanging protons and neutrons. The second part in the word 'isospin' reflects the analogy with the electron spin symmetry, the degeneracy of the spin-up and spin-down electron states in quantum mechanics.

In fact, one introduces a similar formalism in QCD, attributing isospin $I = 1/2$ to the doublet of u and d quarks and treating these two flavours as "up" and "down" components with $I_3 = +1/2$ and $I_3 = -1/2$, respectively. The hadrons containing u and d quarks in different combinations form isomultiplets, with the isospin counting similar to the spin algebra in quantum mechanics. In the case of proton and neutron, the diquark ud has isospin 0, therefore, adding u or d quark to the diquark, we get the nucleon isodoublet ($I = 1/2$) consisting of proton with $I_3 = +1/2$ and neutron with $I_3 = -1/2$. Another isodoublet is formed by K^+ and K^0, where $\bar{s}$ quark, which has no isospin, is combined with u and d, respectively. In the same way, $D^0 (u\bar{c})$ and $D^- (d\bar{c})$, or $B^+ (u\bar{b})$ and $B^0 (d\bar{b})$ build isodoublets.

Note that antiquarks have the opposite signs of I_3: $\bar{u}$ $(\bar{d})$ has $I_3 = -1/2$ $(I_3 = +1/2)$. Combining u and d quark with their antiquarks, one gets four states. Three of them belong to isotriplet ($I = 1$):

$$u\bar{d}\ (I_3 = +1), \quad \frac{u\bar{u} - d\bar{d}}{\sqrt{2}}\ (I_3 = 0), \quad d\bar{u}\ (I_3 = -1). \tag{48}$$

For example, pions (π^+, π^0 and π^-), as well as ρ mesons (ρ^+, ρ^0 and ρ^-) form isotriplets. The fourth quark-antiquark state is an isosinglet ($I = 0$):

$$\frac{u\bar{u} + d\bar{d}}{\sqrt{2}}, \tag{49}$$

which deserves a separate discussion. In general, the $u\bar{u}$ and $d\bar{d}$ states transform into each other via intermediate gluons. In mesons this transition takes place at long distances, due to some nonperturbative mechanism, not necessarily described by diagrams with a fixed number of gluons. In any case, the transition amplitude has a characteristic scale of $O(\Lambda_{QCD})$, much larger than the mass difference $\simeq 2(m_u - m_d)$ between the $u\bar{u}$ and $d\bar{d}$ states. The $\bar{u}u - \bar{d}d$ degeneracy yields two orthogonal physical states, the $I_3 = 0$ component of the isotriplet (48) and the isosinglet (49). Turning to strange quarks one encounters the second $I = 0$ state $\bar{s}s$. The same gluonic transition mechanism provides a mixing between (49) and the $\bar{s}s$-state. Now, the difference between the masses is not small, being of $O(2m_s - 2\tilde{m}) \sim \Lambda_{QCD}$. Hence, the amount of mixing depends on the magnitude of the $s\bar{s} \leftrightarrow (u\bar{u} + d\bar{d})$ transition amplitude. The latter is quite sensitive to the spin-parity of the meson state. For example, the two isosinglet mesons with $J^P = 0^-$ shown in Table 3 have (up to small deviations) the following quark content:

$$\eta(547) \simeq \frac{1}{\sqrt{6}}(u\bar{u} + d\bar{d} - 2\bar{s}s), \tag{50}$$

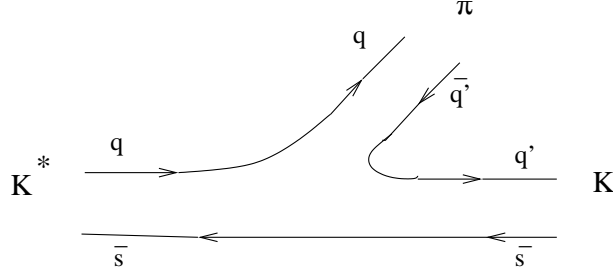$$\eta'(958) \simeq \frac{1}{\sqrt{3}}(u\bar{u} + d\bar{d} + \bar{s}s), \tag{51}$$

Fig. 10: *Quark diagram for $K \to K\pi$ hadronic decays; the four possible combinations of $q = u, d$ and $q' = u, d$ correspond to the four decay modes related by isospin symmetry.*

indicating that mixing in the O^- channel is large. For the $J^P = 1^-$ mesons the situation is completely different. From the quark content of the isosinglet mesons:

$$\omega(782) \simeq \frac{u\bar{u} + d\bar{d}}{\sqrt{2}}, \quad \phi(1020) \simeq \bar{s}s, \tag{52}$$

one concludes that the transition from strange to nonstrange quark pairs in the 1^- state is suppressed.

Returning to the isospin symmetry, it is worth to mention that it yields useful relations between hadronic amplitudes. To give just one simple example, let us consider the four observable hadronic decays of K^*-meson. The amplitudes of these decays are related via isospin symmetry, so that only one amplitude is independent:

$$A(K^{*0} \to K^+\pi^-) = -\frac{1}{\sqrt{2}}A(K^{*0} \to K^0\pi^0) = A(K^{*+} \to K^0\pi^+) = \frac{1}{\sqrt{2}}A(K^{*+} \to K^+\pi^0). \tag{53}$$

To obtain these relations, one does not necessarily need to apply formulae for SU(2) group. In the isospin limit, all four decays are described by a single quark diagram, shown in Fig. 10, where the initial and final mesons are taken in the valence-quark state. Each individual decay mode has its own combination of u and d quarks to be substituted in this diagram. Furthermore, the coefficients $1/\sqrt{2}$ originate from the quark content of π^0. Naturally, the hadronic amplitude attributed to the quark diagram in Fig. 10 is a nonperturbative, long-distance object and cannot be directly calculated in QCD. However all we need are the amplitude relations between individual decay modes and not the value of the amplitude itself. Squaring the relations (53) and taking into account the phase space, one predicts the ratios of branching fractions confirmed by the experimental values given in [4].

2.4 SU(3)-flavour symmetry

Another flavour symmetry, widely used in hadron phenomenology, is $SU(3)_{fl}$ corresponding to the limit of QCD with all three quarks, u,d and s, having equal masses. Since in reality m_s is only inessentially smaller than Λ_{QCD}, the magnitude of $SU(3)_{fl}$-violation in hadrons is not universal, depending on their quark content and quantum numbers.

Neglecting the mass differences between u,d,s quarks and introducing a common mass $\tilde{m}_3$ one approximates L_{QCD} as

$$L_{QCD} \simeq L_{QCD}^{(u=d=s)} = \overline{\Psi}_3(D_\mu\gamma^\mu - \tilde{m}_3)\Psi_3 + L_{glue} + .. , \tag{54}$$

where Ψ_3 is a triplet:

$$\Psi_3 = \begin{pmatrix} \psi_u \\ \psi_d \\ \psi_s \end{pmatrix}, \quad \overline{\Psi}_3 = (\bar{\psi}_u, \bar{\psi}_d, \bar{\psi}_s).$$

The modified QCD with $L_{QCD}^{(u=d=s)}$ has a symmetry with respect to the transitions between 3 flavour states:

$$\Psi_3 \rightarrow \Psi'_3 = \exp\left[-i\sum_{a=1}^{8}\omega^a\frac{\lambda^a}{2}\right]\Psi_3, \quad \bar{\Psi}_3 \rightarrow \bar{\Psi}'_3 = \bar{\Psi}_3\exp\left[i\sum_{a=1}^{8}\omega^a\frac{\lambda^a}{2}\right]. \tag{55}$$

Although physically, $SU(3)_{fl}$ and the fundamental $SU(3)$-colour have completely different origin, the group-theoretical formalism of both symmetries is the same. In particular, the eight λ^a-matrices entering (55) are already given in (8).

The $SU(3)_{fl}$ symmetry is very helpful in "organizing" the spectra of strange and nonstrange hadrons in multiplets. The light-quark meson multiplets are obtained by combining quark flavour-triplets and antiquark flavour-antitriplets. Without using the specific rules of $SU(3)$-algebra, which can be found in many textbooks, it is easy to figure out that the nine quark-antiquark states split into a singlet $\bar{\Psi}_3\Psi_3$ and octet $\bar{\Psi}_3\lambda^a\Psi_3$. The octet has its own isospin substructure [6]. The singlet-octet pattern provides a reasonable description for pseudoscalar mesons, in particular, η' meson is close to the $SU(3)_{fl}$ singlet state (51). The isotriplet of pions (π^+, π^0, π^-), two isodoublets of kaons (K^+, K^0 and $\bar{K}^0, K^-$) and the isosinglet η, given by (50), together form an octet. However, this pattern is not universal. E.g., in the case of vector mesons, ω and ϕ states in (52) are neither octets, nor singlets. To complete the counting of meson $SU(3)_{fl}$ multiplets, one has to mention also triplets and antitriplets of heavy-light mesons. For example, in the case of c quark, $\bar{D}^0, D^-, \bar{D}_s$ (D^0, D^-, D_s) form a triplet (antitriplet).

Generally, $SU(3)_{fl}$ works quite well for baryons, because their characteristic mass scale is a few times larger than Λ_{QCD}. Importantly, the spin-parity of the lowest baryon $SU(3)_{fl}$ multiplets is fixed, due to the total antisymmetry of the baryon "wave-function" in the $SU(3)_{fl}$/spin/colour coordinates required by Fermi-statistics. There is an octet with $J = 1/2$ (including proton and neutron) and decouplet with $J = 3/2$. Let us, for instance, have a look at the latter. It contains the isoquadruplet ($I = 3/2$) of Δ-resonances ($\Delta^{++}(uuu), \Delta^+(uud), \Delta^0(udd), \Delta^-(ddd)$), the isotriplet of Σ resonances ($\Sigma^+(uus)$, $\Sigma^0(uds), \Sigma^-(dds)$), the isodoublet of Ξ-resonances ($\Xi^0(uss), \Xi^-(dss)$) and the isosinglet $\Omega(sss)$. Consulting [4] for the masses of these baryons, one notices a distinct hierarchy: each constituent s quark adds an amount of $O(m_s)$ to the baryon mass.

Returning to the quark diagram in Fig. 10, we may now replace the s quark by u or d quark. In $SU(3)_{fl}$ limit the new diagram obtained after this replacement is equal to the one with s-quark, yielding relations between the $K^* \rightarrow K\pi$ and $\rho \rightarrow \pi\pi$ hadronic amplitudes, e.g.

$$A(K^{*+} \rightarrow K^0\pi^+) \simeq -\frac{1}{\sqrt{2}}A(\rho^+ \rightarrow \pi^0\pi^+). \tag{56}$$

Such relations are typically violated at the level of 20-30 %, but are still useful from the phenomenological point of view.

2.5 Heavy quark symmetry

To complete our survey of flavour symmeties, we now turn to the $\{c, b\}$ quark sector of QCD Lagrangian. The fact that $m_{c,b} \gg \Lambda_{QCD}$, together with the flavour-independence of quark-gluon interactions, allows one to consider an interesting limit of L_{QCD} where both c and b quarks have infinitely heavy mass:

$$m_c \sim m_b \sim m_Q \rightarrow \infty. \tag{57}$$

At first sight, the limit is not justified, because in reality m_b is substantially larger than m_c. As we shall see, the fact that both masses are large turns out to be more important for QCD dynamics. Formally, in the limit (57) one can introduce a doublet of heavy-flavour fields

$$\Psi = \begin{pmatrix} \psi_c \\ \psi_b \end{pmatrix}, \quad \bar{\Psi} = (\bar{\psi}_c, \bar{\psi}_b),$$

---

[6]In mathematical terms $SU(2)_{isospin}$ is a subgroup of $SU(3)_{fl}$.

and rewrite the Lagrangian in a form invariant with respect to SU(2)-rotations in the c, b flavour space:

$$L_{QCD} = \sum_{Q=c,b} \overline{\Psi}_Q(iD_\mu\gamma^\mu - m_Q)\Psi_Q + L_{glue} + L_{u,d,s}\,. \tag{58}$$

This particular form of the heavy-quark limit for L_{QCD} is however not convenient, because the heavy mass scale m_Q is still present explicitly. To understand why it is desirable to effectively remove that scale, let us consider the heavy-quark limit (57) for D or B meson. Since m_c and m_b have no direct relation to QCD, it makes sense to discuss a hypothetical heavy-light meson H with a mass m_H containing a heavy quark with an arbitrarily large mass m_Q. In the rest frame of H the constituent heavy quark stays almost at rest, providing a static source of color charge which emits and absorbs gluon fields. The meson mass, to a good approximation is

$$m_H = m_Q + \bar{\Lambda}\,, \tag{59}$$

where $\bar{\Lambda}$ is the energy of the light quark-gluon "cloud" surrounding the heavy quark. The situation very much resembles the hydrogen atom where the total mass of the atom is a sum of an extremely large ($\sim$ GeV) proton mass and a small energy of the electron cloud ($\sim$ MeV). The essential point is that the electron itself is nonrelativistic. One can isolate the electron mass from the rest of the energy, introduce the Coulomb potential and kinetic energy, and eventually solve the equations of motion, determining the electron energy levels. In heavy hadrons the light-quark cloud is purely relativistic ($m_{u,d,s} < \Lambda_{QCD}$) and has a complicated long-distance nature.

Nevertheless, one essential feature is common for both bound states. In the atom the energy of the electron cloud does not depend on the proton mass. Likewise, in the heavy-light meson $\bar{\Lambda}$ in (59) is (up to $1/m_Q$ corrections) independent of m_Q. From atomic physics we know that the electron energy levels in hydrogen and deuterium coincide to a great precision. The fact that deuteron is twice more massive than proton, does not play a role for the energy levels, because in both cases the atomic nuclei are static. Important is that the electric charge does not change by switching from proton to deuteron. Similarly, in the H meson $\bar{\Lambda}$ changes very little if one replaces m_Q by m_b or by m_c, because the colour charge of the heavy quark does not change. Thus, the heavy-flavour symmetry is in reality the symmetry between the light-quark remnants of the heavy hadrons, so that the heavy-quark mass scale indeed plays a secondary role.

To achieve a quantitative level, a special formalism of *heavy quark effective theory* (HQET) was developed for applications of QCD to heavy-light hadrons. One starts from L_{QCD} and introduces transformations which decouple the $\sim m_Q$ part of the heavy-quark field from the part which has the remnant momentum $\sim \Lambda_{QCD}$. Only the latter part strongly interacting with the light quark-gluon cloud is relevant for QCD dynamics. In HQET one integrates out the heavy degrees of freedom and works with the Lagrangian containing a new effective quark field carrying the flavour of Q but no mass. Not only the static limit (57) but also an expansion in powers of $1/m_Q$ can be systematically treated. The field-theoretical aspects of heavy-mass expansion are nicely explained in the literature (see e.g., [8],[9]); I will only focus on some important phenomenological consequences of heavy-flavour symmetry.

One famous example is the $B \to Dl\nu_l$ decay involving weak $b \to c$ transition in Standard Model. The unknown part of the decay amplitude is the hadronic matrix element

$$\langle D(p_D)|\bar{c}\gamma_\mu b|B(p_B\rangle \tag{60}$$

determined by the long-distance interactions involving the initial and final heavy quarks as well as the surrounding light quark-gluon "cloud". One chooses a special kinematical configuration, the "zero recoil point" where the momentum transfer to the lepton pair is equal to

$$q^2 = (p_B - p_D)^2 = (m_B - m_D)^2\,. \tag{61}$$

In the B meson rest system $p_B = (m_B, 0, 0, 0)$ this point correspond to the final D meson at rest. In the heavy-quark limit the replacement of b quark by c-quark does not change the hadronic state:

$$\langle D(p_D)| = \langle B(p_B)|$$

and the matrix element (61) reduces to a trivial normalization factor. One can therefore predict the decay amplitude in the zero recoil point up to $1/m_Q$ corrections. In fact there is a theorem stating that these corrections are even smaller and start from $O(1/m_Q^2)$, but to derive this and other important details one needs a full-scale HQET framework.

Without resorting to the effective theory, it is possible to understand the origin of another important symmetry emerging in the heavy-quark limit. In the hydrogen atom, the electron and proton have magnetic moments related to their spins and yielding interactions with the external magnetic fields or with each other (spin-spin interactions). The magnetic moments are inversely proportional to the masses, so that the proton magnetic moment plays no role for the electron energy levels. Each level is degenerate with respect to the proton spin direction. Since QED and QCD have very similar vector boson interactions with spin 1/2 particles, the spin 1/2 quarks also have *chromomagnetic* moments. and interact with the "magnetic" parts of gluonic fields and with other quarks. For the heavy nonrelativistic quark the chromomagnetic moment is inversely proportional to the heavy quark mass m_Q. In the infinite mass limit the interaction vanishes and, hence the light-cloud energy $\bar{\Lambda}$ is independent of the spin orientation of the heavy quark.

One arrives at a new classification of heavy-light states based on this *heavy-quark spin symmetry*. Instead of adding together the orbital momentum and the total spin of quarks as we did in (42) it is more appropriate to introduce, for a $Q\bar{q}$ meson ($Q = c, b$; $q = u, d, s$), the total angular momentum of light degrees of freedom:

$$\vec{J}_{light} = \vec{L} + \vec{s}_q \tag{62}$$

Adding the heavy quark spin $s_Q = 1/2$ to J_{light} one gets degenerate doublets of heavy-light mesons with total angular momentum $J = J_{light} \pm 1/2$. At $L = 0$ one simply has $J_{light} = 1/2$ and therefore a doublet of mesons with $J^P = 1^-$ and $J^P = 0^-$ consisting of B and B^* (D and D^*) in the b quark (charm) sector. The mass differences within doublets are indeed very small [4]:

$$\delta_B = m_{B^*} - m_B = 47 \text{ MeV}, \quad \delta_D = m_{D^*} - m_D = 142 \text{ MeV}, \tag{63}$$

indicating that the heavy-quark spin symmetry works quite well, especially for the heavier b quark. Taking into account that the mass differences are $\sim 1/m_Q$ effects, one expects that $\delta_B/\delta_D \simeq (m_c/m_b)$ which is also in accordance with (63) and (31). I leave as an exercise to show that at $L = 1$ there are two degenerate doublets: one with $J^P = 0^+, 1^+$ and another one with $J^P = 2^+, 1^+$.

2.6 Exotic hadrons

The colour confinement principle does not exclude hadronic states with an "exotic" valence quark content, different from $q\bar{q}$ or qqq. Quarks, antiquarks and gluons can be added together in any combination, e.g., $q\bar{q}G$, GG, $q\bar{q}q\bar{q}$ or $q\bar{q}qq$, provided they are in a colour-neutral state. Since one cannot calculate the spectrum of hadrons in QCD with a good precision, predictions of exotic states are generally model-dependent. It is always problematic to distinguish an exotic hadron from the excitation of an ordinary hadron with the same J^P and flavour quantum numbers. Moreover, in this case one expects mixing between ordinary and exotic hadrons. For example, if there is a $J^P = 0^-$ state composed of two gluons GG (*glueball*), it should be mixed with η' to a certain degree, so that η' acquires a glueball component.

Therefore, the most interesting, "smoking gun" signatures are the hadrons with exotic quantum numbers (flavour content and/or J^{PC}), forbidden for quark-antiquark mesons or three-quark baryons. For example it is impossible to arrange a flavour-neutral quark-antiquark state with $J^{PC} = 1^{-+}$. The P and C (charge-conjugation) parities of a fermion-antifermion state are determined by the rules: $P =$
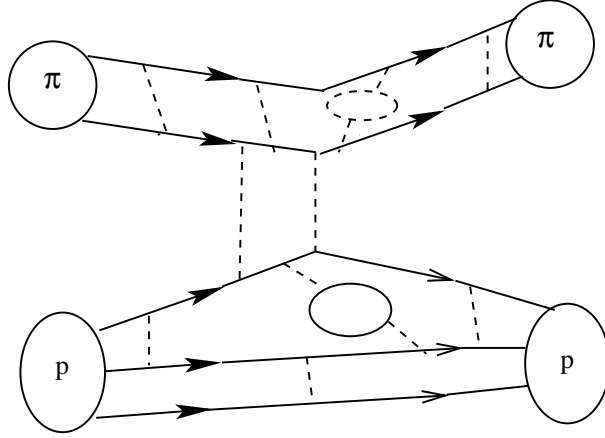
Fig. 11: *A schematic view of pion-proton elastic scattering at large momentum transfers.*

$-(-1)^L$ and $C = (-1)^{L+S}$, so that $P = -1$ means $L = 0, 2, ...$ Hence, the only possibility to have $C = +1$ is $S = 0, 2, ...$ However, adding together even values of L and S one cannot get $J = 1$. On the other hand, adding one constituent gluon to a $q\bar{q}$ pair, one easily makes a "hybrid" meson with $q\bar{q}G$ content and $J^{PC} = 1^{-+}$ quantum numbers. Searches for hybrid mesons are currently being carried out, but the experimental situation is not yet settled.

The recently observed narrow baryon resonance $\Theta(1540)$ decaying to $K^+ n$[10] is another promising candidate for hadron exotics, a state $\bar{s}uudd$ with five valence constituents (*pentaquark*). Flavour symmetries are important model-independent tools to confirm/reject the experimental candidates for exotic resonances. In particular, an important task is to find the symmetry partners of these hadrons and to fill the relevant isospin and $SU(3)_{fl}$ multiplets (in case of the pentaquark it is actually the $SU(3)_{fl}$ antidecouplet).

3. QCD AT SHORT DISTANCES

3.1 Probing short distances with electroweak quark currents

In this lecture we return to the quark-gluon interactions at large momentum transfers (short distances). In this region, practically at $Q \geq 1$ GeV, α_s is small, allowing one to apply the perturbative expansion. It is then possible to test QCD quantitatively, calculating various quark-gluon interaction processes at large Q and comparing the results with the available experimental data. Note however, that the traditional way to study interactions by scattering one object on the other is not applicable to quarks and gluons. They simply are not available in free-particle states. One needs to trace quarks inside hadrons, where the long-distance forces are important. Take as an example the elastic pion-proton scattering at large momentum transfers (see Fig. 11). Here one has to combine the perturbative quark-quark scattering amplitudes (two-gluon exchange) with the "wave functions" of quarks inside the initial and final hadrons. To obtain these functions one needs to go beyond perturbative QCD. Therefore, an unambiguous extraction of the perturbative amplitude from the data on the scattering cross section is not a realistic task.

The situation is not so hopeless, actually, since we have at our disposal electroweak bosons (γ, W, Z) interacting with quarks in a pointlike way. Electroweak interactions at large momentum transfer serve as external probes of short-distance dynamics. In Lecture 1, we already discussed one example: the quark-antiquark pair production in Z decay. To list all possible electroweak sources of quarks in a more systematic way, I start with the photon. Its interaction with the quark e.m. current was already given in (6), let me write it down again:
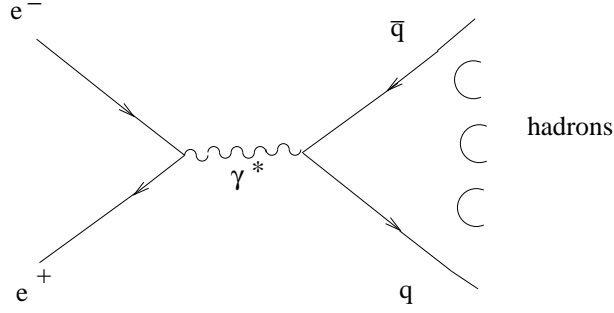
$$L_{em}(x) = -e j_\mu^{em} A^\mu \, , \tag{64}$$

Fig. 12: *The virtual-photon exchange diagram for* $e^+e^- \rightarrow hadrons$

introducing a compact notation for the quark e.m. current:

$$j_\mu^{em} = \sum_{q=u,d,s,c,..} Q_q \bar{\psi}_q \gamma_\mu \psi_q \,, \tag{65}$$

where the summation over colour indices is not shown for brevity. The quark weak current entering the quark-W flavour-changing interaction:

$$L_W(x) = -\frac{g}{2\sqrt{2}} j_\mu^W W^\mu + c.c. \tag{66}$$

is more complicated and includes the CKM mixing matrix:

$$j_\mu^W(x) = (\bar{u},\bar{c},\bar{t})\gamma_\mu(1-\gamma_5) \begin{pmatrix} V_{ud} & V_{us} & V_{ub} \\ V_{cd} & V_{cs} & V_{cb} \\ V_{td} & V_{ts} & V_{tb} \end{pmatrix} \begin{pmatrix} d \\ s \\ b \end{pmatrix} . \tag{67}$$

Finally, the quark-Z interaction is

$$L^Z = -\frac{g}{2cos\theta_W} j_\mu^Z Z_\mu \,, \tag{68}$$

where the quark electroweak neutral current is a mixture of vector and axial-vector parts.

3.2 Perturbative QCD in $e^+e^- \rightarrow hadrons$

In e^+e^- annihilation at high energies the virtual photon provides a short-distance source of quark-antiquark pairs. This process is hadron-free in the initial state. The photon-exchange diagram is depicted in Fig. 12 (for simplicity, I ignore the additional Z-exchange diagram). The experimentally measured total cross section $\sigma_{tot}(e^+e^- \rightarrow h)$ depends on one kinematical variable $s = (p_{e^-} + p_{e^+})^2$. The virtual timelike photon transfers its energy $\sqrt{s}$ to the hadronic state. At very large $\sqrt{s} \gg \Lambda_{QCD}$ and $\sqrt{s} \gg m_q$, the initial pair of quarks is produced at an average distance of $O(1/\sqrt{s})$, much smaller than the typical hadronic distance scale $1/\Lambda_{QCD}$. Due to asymptotic freedom of QCD, gluonic interactions of the produced quark pair are suppressed by small α_s. Hence, e^+e^- annihilation at high energies provides an almost pointlike source of quasi-free quark pairs. At long distances the created quarks and antiquarks are inevitably converted into some hadronic state. Since in the total cross section the summation is done over all hadronic states produced at a given energy, the total probability of hadronization sums up to a unit. Hence, at $\sqrt{s} \rightarrow \infty$ the hadronic cross section is well approximated by the cross section of the free quark-antiquark pair production:

$$\sigma_{tot}^{(e^+e^- \rightarrow h)}(s) \simeq \sum_{q=u,d,s,..} \sigma^{(e^+e^- \rightarrow q\bar{q})}(s) \,, \tag{69}$$

summed over all quark flavours with $m_q \ll \sqrt{s}$. This, so called *parton model* approximation for $e^+e^- \to h$ is confirmed by experimental data. Moreover, the majority of events saturating the cross section at high $\sqrt{s}$ consists of two distinct hadronic jets originating from the initial quark pair.

The way we obtained (69) may seem too qualitative and a bit "hand-waving". In the following, we shall derive the asymptotic cross section (69) in a more rigorous way. In this derivation several important concepts will be introduced, to be used in discussing further topics covered by these lectures.

We start with the formal definition of the total cross section:

$$\sigma_{tot}^{(e^+e^- \to h)}(s) = \frac{1}{2s} \sum_{h_n} |\langle h_n \mid T \mid e^+e^- \rangle|^2 \,, \tag{70}$$

where the sum over the final hadronic states h_n includes phase-space integration and implies summation over spins (polarizations). The matrix elements $\langle f|T|i\rangle \equiv T_{fi}$ (in (70) $|i\rangle = |e^+e^-\rangle$ and $\langle f| = \langle h_n|$) determine the general S-matrix of the theory:

$$S_{fi} \equiv \langle f|S|i\rangle = \delta_{fi} + iT_{fi} \,. \tag{71}$$

The usual representation of S-matrix in terms of Lagrangian has the time-ordered exponential form:

$$S = T\left\{ \exp\left[i \int d^4x \left(L_{QCD}(x) + L_{QED}(x) \right) \right] \right\} \,, \tag{72}$$

where L_{QED} includes e.m. interactions of quarks and leptons. Furthermore, the unitarity of S matrix is used:

$$SS^\dagger = 1 \,, \tag{73}$$

or

$$\sum_n \langle f|S|n\rangle \langle n|S^\dagger|i\rangle = \delta_{fi} \,. \tag{74}$$

From now on we consider the forward scattering $f = i$. Replacing $\langle n|S^\dagger|i\rangle = \langle i|S|n\rangle^*$ and substituting (71) in (74), one obtains the unitarity relation for T_{ii} (the optical theorem):

$$2\mathrm{Im} T_{ii} = \sum_n |T_{ni}|^2 \,. \tag{75}$$

To apply this universal relation to e^+e^-- scattering, we take $|i\rangle = |e^+e^-\rangle$ with four-momentum $q = p_{e^+} + p_{e^-}$, so that $q^2 = s > 0$. Furthermore, we choose $|n\rangle = |h_n\rangle$ restricting the set of intermediate states by hadronic states. As a result we obtain a rigorous relation between the amplitude of the forward $e^+e^- \to h \to e^+e^-$ scattering via hadronic intermediate states, $T_{ii} = \mathcal{A}^{(e^+e^- \to h \to e^+e^-)}$, and the sum over the squared $e^+e^- \to h_n$ amplitudes. The latter sum, according to (70) is proportional to the total hadronic cross section. The optical theorem (75) takes the form:

$$2\,\mathrm{Im}\,\mathcal{A}^{(e^+e^- \to h \to e^+e^-)}(s) = \sum_{h_n} |\langle h_n|T|e^+e^-\rangle|^2 = 2s\sigma_{tot}^{(e^+e^- \to h)}(s)\,. \tag{76}$$

Diagrammatically, this relation is represented in Fig. 13. The amplitude

$$\mathcal{A}^{(e^+e^- \to h \to e^+e^-)}(q^2) = \frac{e^4}{(q^2)^2}(\bar{\psi}_e \gamma^\mu \psi_e)(\bar{\psi}_e \gamma^\nu \psi_e)\Pi_{\mu\nu}(q) \tag{77}$$

contains the photon propagators and the products of electron and positron spinors in both initial and final states, written according to the QED Feynman rules. The nontrivial part of this amplitude, denoted as $\Pi_{\mu\nu}$, describes the $j_\mu^{em} \to h \to j_\nu^{em}$ transition, and is called the *correlation function* (or correlator) of quark currents. The formal expression for this object reads:

$$\Pi_{\mu\nu}(q) = i \int d^4x \, e^{iqx} \langle 0|T\{j_\mu^{em}(x)j_\nu^{em}(x)\}|0\rangle \,. \tag{78}$$
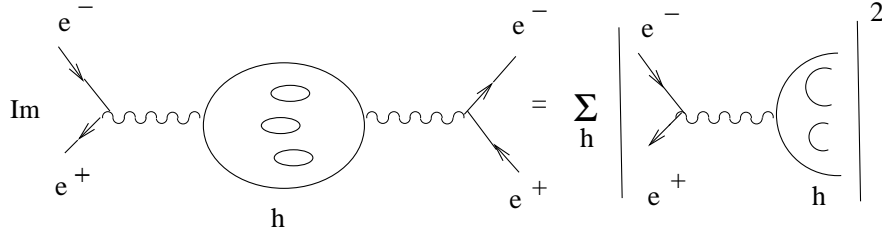
Fig. 13: *Unitarity relation for $e^+e^- \to hadrons$*

Due to the conservation of e.m. current ($\partial^\mu j_\mu^{em} = 0$), the correlation function depends on one invariant amplitude:

$$\Pi_{\mu\nu}(q) = (-g_{\mu\nu}q^2 + q_\mu q_\nu)\Pi(q^2). \tag{79}$$

Substituting (79) in (77) and taking imaginary part from both sides, we obtain

$$\operatorname{Im} \mathcal{A}^{(e^+e^- \to h \to e^+e^-)}(s) = -\frac{e^4}{s}(\bar{\psi}_e\gamma^\mu\psi_e)(\bar{\psi}_e\gamma_\mu\psi_e)\operatorname{Im}\Pi(s). \tag{80}$$

It is convenient to normalize the hadronic cross section to the $e^+e^- \to \mu^+\mu^-$ cross section known from QED. One can literally repeat the derivation done above, taking instead of hadronic states the $\mu^+\mu^-$ states: $|n\rangle = |\mu^+\mu^-\rangle$. The resulting relations are quite similar to (76), (77) and (80):

$$2\operatorname{Im} \mathcal{A}^{(e^+e^- \to \mu^+\mu^- \to e^+e^-)}(s) = \sum_{\mu^+\mu^-} |\langle \mu^+\mu^-|T|e^+e^-\rangle|^2 = 2s\sigma^{(e^+e^- \to \mu^+\mu^-)}(s), \tag{81}$$

$$\mathcal{A}^{(e^+e^- \to \mu^+\mu^- \to e^+e^-)}(q^2) = \frac{e^4}{(q^2)^2}(\bar{\psi}_e\gamma^\rho\psi_e)(\bar{\psi}_e\gamma^\lambda\psi_e)\Pi_{\rho\lambda}^{(\mu)}(q), \tag{82}$$

and

$$\operatorname{Im} \mathcal{A}^{(e^+e^- \to \mu^+\mu^- \to e^+e^-)}(s) = -\frac{e^4}{s}(\bar{\psi}_e\gamma^\mu\psi_e)(\bar{\psi}_e\gamma_\mu\psi_e)\operatorname{Im}\Pi^{(\mu)}(s), \tag{83}$$

where the muonic correlation function $\Pi^{(\mu)}$ is nothing but a 2-point muon-loop diagram. Furthermore, the cross section in (81) taken from QED textbooks, reads:

$$\sigma^{(e^+e^- \to \mu^+\mu^-)}(s) = \frac{4\pi\alpha_{em}^2}{3s}. \tag{84}$$

Dividing the hadronic unitarity relation (76) by the muonic one (81) and using (80) and (83), we obtain a useful ratio:

$$\frac{\operatorname{Im}\Pi(s)}{\operatorname{Im}\Pi^{(\mu)}(s)} = \frac{\sigma_{tot}^{(e^+e^- \to h)}(s)}{\sigma^{(e^+e^- \to \mu^+\mu^-)}(s)} \equiv R(s). \tag{85}$$

The next key point in our derivation is the analysis of the correlation function $\Pi(q^2)$ at spacelike $q^2 < 0$. At large $|q^2| = Q^2 \gg \Lambda_{QCD}^2$, the long-distance domain in the space-time integral in (78) is suppressed by the strongly oscillating exponent and the short distances/times $|\vec{x}| \sim x_0 \sim 1/Q$ dominate. This justifies using QCD perturbation theory with $\alpha_s(Q) \to 0$ at $Q \to \infty$. The leading-order

(a)

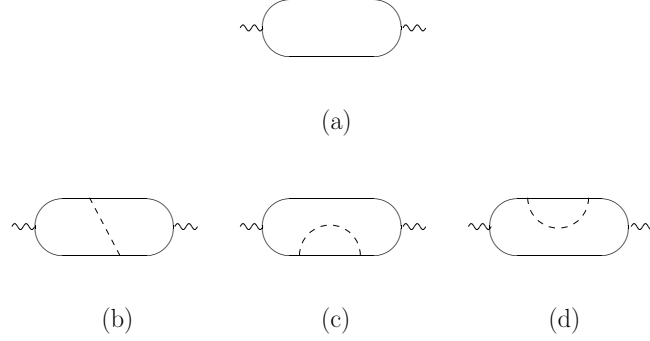(b)   (c)   (d)

Fig. 14: *Diagrams corresponding to the perturbative contributions to the correlation function of two quark currents: (a) the leading-order loop and (b-d) the $O(\alpha_s)$ corrections. Wavy lines denote external currents with 4-momentum q, solid lines quarks and dashed lines gluons.*

asymptotically free result is given by the 2-point quark-loop diagram (Fig. 14a), and the next-to-leading corrections are determined by $O(\alpha_s)$ two-loop diagrams (Fig. 14b,c,d). Calculation of these diagrams yields (at $m_q \ll Q$):

$$\Pi(q^2) = -\frac{1}{4\pi^2}\left(\sum_q Q_q^2\right)\log\left(\frac{-q^2}{\mu^2}\right)\left(1 + \frac{\alpha_s}{\pi}\right) + O\left(\frac{1}{\epsilon}\right) + const\,, \tag{86}$$

where each flavour q contributes with the same expression and a coefficient Q_q^2. The natural scale for α_s is q^2. In recent years, due to tremendous calculational efforts, the $O(\alpha_s^2)$ and even $O(\alpha_s^3)$ corrections to Π have been calculated; also the loop diagrams for the massive quark are known with a high accuracy.

In the final stage of our derivation the calculated function $\Pi(q^2)$ at $q^2 < 0$ is related to $\mathrm{Im}\Pi(s)$ at positive s. One employs Cauchy theorem for the function $\Pi(z)$ obtained from $\Pi(q^2)$ by analytically continuing the real variable q^2 to the complex values, $q^2 \to z$:

$$\Pi(q^2) = \frac{1}{2\pi i}\int_C dz\frac{\Pi(z)}{z - q^2}\,. \tag{87}$$

The integration contour C is shown in Fig. 15. It circumvents the singularities of the function $\Pi(z)$, i.e. the points/regions where $\mathrm{Im}\Pi(z) \neq 0$. According to (76) and (80) the location of singularities at real $q^2 > 0$ is determined by the masses of resonances and/or the thresholds of multiparticle hadronic states produced in $e^+e^- \to h$; the lowest one is at $s_{min} = 4m_\pi^2$ corresponding to the threshold of the lightest two-pion state. Subdividing the contour C into: 1) a large circle with the radius R, 2) an infinitely small semicircle $\tilde{C}$ surrounding s_{min} and 3) two straight lines from s_{min} to R, we can rewrite the integral in terms of three separate contributions:

$$\Pi(q^2) = \frac{1}{2\pi i}\int_{|z|=R} dz\frac{\Pi(z)}{z - q^2} + \frac{1}{2\pi i}\int_{s_{min}}^R dz\frac{\Pi(z + i\delta) - \Pi(z - i\delta)}{z - q^2} + \frac{1}{2\pi}\int_{\tilde{C}} dz\frac{\Pi(z)}{z - q^2}\,. \tag{88}$$

Suppose the function decreases at $|q^2| \to \infty$: $\Pi(q^2) \sim 1/|q^2|^\lambda$, where $\lambda > 0$. Then the first integral vanishes at $R \to \infty$. Taking infinitely small semicircle, one makes the third integral also vanishing. Furthermore, since there are no singularities of $\Pi(z)$ at $\mathrm{Re}z < s_{min}$, the integrand in the second integral reduces to the imaginary part: $\Pi(q^2 + i\delta) - \Pi(q^2 - i\delta) = 2i\mathrm{Im}\Pi(q^2)$ (due to Schwartz reflection
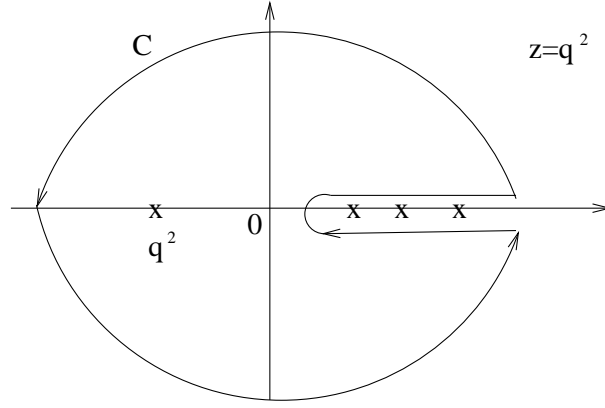
Fig. 15: *The integration contour in (87). The crosses on the positive real axis indicate singularities of $\Pi(q^2)$*

principle). Finally, we obtain the desired *dispersion relation*

$$\Pi(q^2) = \frac{1}{\pi} \int\limits_{s_{min}}^{\infty} ds \frac{\mathrm{Im}\Pi(s)}{s - q^2 - i\delta} \tag{89}$$

with l.h.s. calculated in QCD in a form of perturbative expansion (86) and r.h.s. related to the cross section via (85):

$$\mathrm{Im}\Pi(s) = R(s)\mathrm{Im}\Pi^{(\mu)}(s). \tag{90}$$

The quantity $R(s)$ is directly measurable in e^+e^- experiments. It remains to determine $\mathrm{Im}\Pi^{(\mu)}(s)$. Knowing the answer for the quark loop diagram in Fig. 14a it is very easy to write down the expression for the muon loop. Since we neglect masses in both diagrams, the only difference is the factor 3, from summing up the colour states in the quark loop. This factor is naturally absent for the muon loop. From (86), taking imaginary part, one obtains

$$\mathrm{Im}\Pi^{(\mu)}(s) = \frac{1}{12\pi}. \tag{91}$$

Finally, to guarantee the convergence of the dispersion integral (89), [7] let us differentiate both parts in q^2:

$$\frac{d\Pi(q^2)}{dq^2} = \frac{1}{\pi} \int\limits_{s_{min}}^{\infty} ds \frac{\mathrm{Im}\Pi(s)}{(s - q^2)^2}. \tag{92}$$

where (86) gives for l.h.s.

$$\frac{d\Pi(q^2)}{dq^2} = \left(\sum_q^{n_f} Q_q^2\right)\left(-\frac{1}{4\pi^2 q^2}\right)\left(1 + \frac{\alpha_s}{\pi}\right). \tag{93}$$

Note that divergent and constant terms disappeared after differentiation and play no role in our derivation. The final form of the dispersion relation is

$$\frac{3\left(\sum_q^{n_f} Q_q^2\right)}{-q^2}\left(1 + \frac{\alpha_s}{\pi} + ...\right) = \int\limits_{s_{min}}^{\infty} ds \frac{R(s)}{(s - q^2)^2}, \tag{94}$$

---

[7]For brevity, I avoid a longer derivation which includes some special mathematical construction (subtractions).
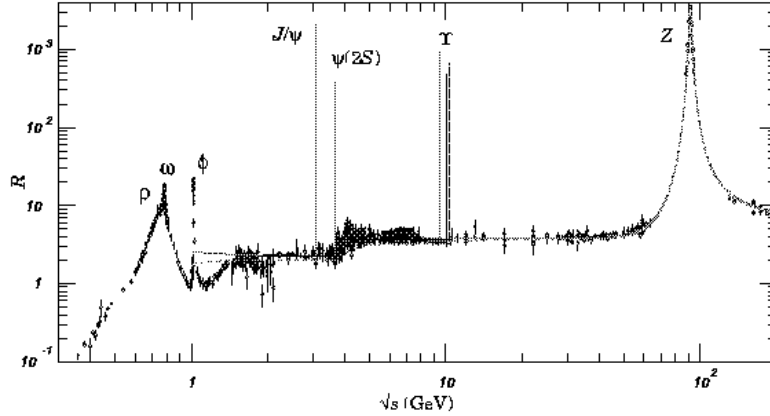
Fig. 16: *Ratio R from [4]*

where ellipses denote higher-order in α_s corrections. The fact that (94) is valid at $(-q^2) \to \infty$ unambiguously fixes the constant limit of $R(s)$ at large s:

$$R(s) \to 3 \sum_q^{n_f} Q_q^2 \,, \tag{95}$$

where n_f indicates that R includes all "active" quark flavours, for which the condition $\sqrt{s} \gg m_q$ is fulfilled. Finally, we notice that (95) coincides with the parton model prediction (69), taking into account that the free-quark- and muon-pair cross sections differ only by the colour factor times the quark charge squared:

$$\sigma^{(e^+ e^- \to q\bar{q})}(s) = 3 Q_q^2 \sigma^{(e^+ e^- \to \mu^+ \mu^-)}(s) \,.$$

Importantly, QCD not only reproduces the parton model prediction for $R(s)$ but also provides perturbative corrections, as well as predicts the integral (94) over $R(s)$.

The experimental data collected in various regions of $\sqrt{s}$ nicely confirm (95). According to Fig.16 taken from [4], the ratio $R(s)$ approaches first the constant value $R \simeq 2$ at energies $\sim 2 - 3$ GeV, above the region of vector meson resonances ρ,ω,ϕ (and below the charm threshold). That is exactly the value anticipated from (95) for $n_f = 3$. Well above charmonium resonances, a new constant level is achieved: $R = 2 + 3 Q_c^2 = 10/3$. And finally, $R = 10/3 + 3 Q_b^2 = 11/3$ is settled at energies above Υ resonances, where all five quark flavours are in their asymptotic regime. Actually, the current data on $R(s)$ are so precise that one should also include small α_s-corrections to R_{QCD}.

There are other similar inclusive observables calculable in QCD, among them the total widths $\Gamma_{tot}(Z \to hadrons)$ and $\Gamma_{tot}(W \to hadrons)$. They have the same status as $R(s)$, but a fixed scale m_Z or m_W instead of $\sqrt{s}$. One has also to mention an interesting and well developed sub-field of perturbative QCD related to the jet and/or heavy-quark production in $e^+ e^-$ and hadron collisions at high energies. The underlying short-distance quark-gluon processes are successfully traced in the experimentally observed multijet structure of the final state. Naturally, hadrons cannot be completely avoided, because, after all, quarks and gluons hadronize. In fact, hadronization in jet physics is nowadays a somewhat routine procedure described by QCD-oriented models (e.g. the Lund model integrated within PYTHIA [11]). At lower scales, $Q \sim 1 - 2$ GeV, inclusive decays of τ-lepton are among useful tools to study perturbative QCD (see, e.g. [12]).

3.3 Deep inelastic scattering and operator-product expansion

The processes of lepton-nucleon *deep inelastic scattering* (DIS), $lN \rightarrow lh$ and $\nu_l N \rightarrow lh$ ($l = e, \mu$), are among the best testing grounds of QCD. The long-distance structure of the initial nucleon makes these processes more complicated than $e^+ e^- \rightarrow hadrons$. For definiteness, let us consider the electron-nucleon scattering mediated by the virtual photon γ^* with the 4-momentum q, whereas p is the nucleon 4-momentum. To measure the DIS cross section, one only has to detect the final electron. In the nucleon rest frame the invariant variables $Q^2 = -q^2$ and $\nu = q \cdot p$ are related to the initial and final energies and the scattering angle of the electron: $Q^2 = 4EE' sin^2\theta$, $\nu = (E - E')m_N$.

The specific kinematical region $Q^2 \sim \nu \gg \Lambda_{QCD}^2$ has to be chosen to reveal the spectacular effect of asymptotic freedom. In this region the experimentally measured DIS cross section, normalized to the cross section of the electron scattering on a free pointlike quark σ_{point}, depends essentially on the ratio $x = Q^2/2\nu$. This effect (*Bjorken scaling*), was first interpreted in terms of a beautiful phenomenological model suggested by Feynman. One considers the reference frame with large nucleon momentum p, so that $-\vec{q}$ gives the longitudinal direction. Neglecting long-distance binding forces between quarks, the initial nucleon is represented as a bunch of free constituents (*partons*): quarks, antiquarks and gluons moving in the longitudinal direction [8]. For simplicity the quark masses and transverse momenta as well as the nucleon mass are neglected, in comparison with Q^2 and ν. The electron scatters on one of the nucleon constituents (excluding gluons, of course, because they are electrically neutral) which has the momentum fraction ξ, so that after the pointlike collision the quark 4-momentum is $p\xi + q$. The massless quark has to remain on-shell, $(\xi p + q)^2 = 0$, therefore $2\xi(p \cdot q) + q^2 = 0$ and

$$\xi = Q^2/2\nu = x. \tag{96}$$

The cross section is then represented as a sum of all possible "elementary" processes integrated over ξ

$$d\sigma^{(eN \rightarrow eh)}(Q^2, \nu) = \int_0^1 \sum_{i=u,\bar{u},d,\bar{d}...} f_i(\xi) d\sigma_{point}^i(Q^2, \nu)\delta(\xi - x)d\xi = \sum_i d\sigma_{point}^i(Q^2, \nu)f_i(x), \tag{97}$$

where δ-function takes into account (96). The sum goes over all quark and antiquark species inside proton, and $f_i(\xi)$ are the *parton distributions* defined as the probabilities to find the i-th constituent with the momentum fraction ξ.

In QCD, the scaling behaviour (97) corresponds to the asymptotic-freedom approximation ($\alpha_s = 0$). Switching on the perturbative quark-gluon interactions one predicts logarithmic corrections $\sim log(Q^2)$ to this formula which are nicely reproduced by experiment. There are many excellent reviews and lectures where DIS in perturbative QCD are discussed (see e.g.[13]). Here we shall concentrate on one essential aspect: separation of long- and short-distance effects.

Let us approach DIS from the quantum-field theory side, as we did above for $e^+ e^- \rightarrow hadrons$. Omitting for simplicity the initial and final electrons, one can represent the hadronic part of the DIS cross section in a form of $\gamma^* N \rightarrow h$ cross section. Employing unitarity relation (75) with $|i\rangle = |\gamma^* N\rangle$ one is able to relate the DIS cross section to the $\gamma^*(q)N(p) \rightarrow \gamma^*(q)N(p)$ forward-scattering amplitude (see Fig. 17):

$$2 \, \text{Im} \, \mathcal{A}^{(\gamma^* N \rightarrow h \rightarrow \gamma^* N)}(q, p) = \sum_{h_n} |\langle h_n|T|\gamma^* N\rangle|^2 \sim d\sigma^{(\gamma^* N \rightarrow h)}(Q^2, \nu). \tag{98}$$

The amplitude

$$\mathcal{A}^{(\gamma^* N \rightarrow h \rightarrow \gamma^* N)}(q, p) = \epsilon^\mu(q)\epsilon^\nu(q)T_{\mu\nu}(q, p) \tag{99}$$

contains the photon polarization vectors multiplied by a new purely hadronic object

$$T_{\mu\nu}(p, q) = i \int d^4x e^{iqx} \langle N(p)|T\{j_\mu^{em}(x)j_\nu^{em}(0)\}|N(p)\rangle, \tag{100}$$

---

[8]We refer here to a generic picture of the nucleon, where all possible multiparticle components are coherently added to the valence three-quark state, similar to (41) for the pion.
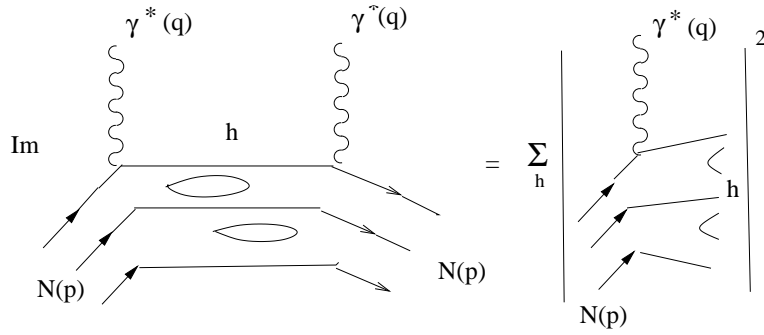
Fig. 17: *Unitarity relation for DIS cross section*

which resembles the correlation function of two currents we introduced above, but, instead of vacuum, has nucleons in the initial and final states.

One can prove that at large Q^2 and ν the dominant contribution to the above integral stems from small space-time intervals $x^2 \sim 1/Q^2 \sim 1/\nu$ [9]. In other words, the points of absorption and emission of the virtual photon are located close to the light-cone $x^2 = 0$. The process takes place in the asymptotic freedom regime, that is, a single quark absorbs the photon, and penetrates quasi-freely at small x^2 before emitting the photon. All other contributions, for example, with different quarks emitting and absorbing initial and final photons are suppressed by powers of $1/Q^2, 1/\nu$. To describe the free-quark propagation from x to 0 we use the quark propagator

$$\langle 0|T\{\psi_q(x)\bar{\psi}_q(0)\}|0\rangle = \int d^4p \left(\frac{p_\alpha \gamma^\alpha}{p^2}\right) e^{-ipx} = \frac{ix_\alpha \gamma^\alpha}{2\pi^2(x^2)^2} \,. \tag{101}$$

neglecting the quark mass. Substituting the e.m. currents in (99) in terms of quark fields, contracting the fields of the propagating quark and using (101) we obtain

$$T_{\mu\nu}(p,q) = i \int d^4x e^{iqx} \sum_{q=u,d,s,..} \langle N(p)|T\{\bar{\psi}_q(x)\gamma_\mu\psi_q(x)\bar{\psi}_q(0)\gamma_\nu\psi_q(0)\}|N(p)\rangle$$

$$= i \int d^4x e^{iqx} \frac{ix_\alpha}{2\pi^2(x^2)^2} \sum_{q=u,d,s,..} \langle N(p)|\bar{\psi}_q(x)\gamma_\mu\gamma_\alpha\gamma_\nu\bar{\psi}_q(0)|N(p)\rangle + \dots \tag{102}$$

In this expression, where only the leading term is shown, the calculable short-distance part (the quark propagator) is separated from the long-distance part which is represented by the quark-antiquark matrix element taken between nucleon states. This hadronic matrix element is a complicated object which has to be either determined from experiment or calculated using methods beyond perturbative QCD which will be discussed in the next two lectures. I skip the derivation of the cross section formula from the imaginary part of $T_{\mu\nu}$ which allows to relate the matrix element introduced in (102) with the parton distributions. Also α_s corrections can be systematically calculated; they contain important and observable $logQ^2$ effects. Important is that the long-distance matrix element (or parton distributions) are universal characteristics of the nucleon and they do not change if the short-distance part of the process changes (e.g., by switching to neutrino-nucleon scattering $W^*N \to h_c$ where the charmed quark is produced). To

---

[9]Note that the light-cone dominance $x^2 = x_0^2 - \vec{x}^2 \sim 0$ is a more general condition than the small-distance/time dominance $x_0 \sim \vec{x} \sim 0$ which takes place in $e^+e^- \to hadrons$.

summarize, in DIS it is possible to separate the short-distance domain by choosing appropriate kinematical region and defining convenient physical observables. The short-distance quark-gluon interactions are calculable in a form of perturbation theory in α_s, whereas the long-distance part is parameterized in terms of universal hadronic matrix elements. The procedure of approximating the product of currents in (102) by a quark-antiquark operator and separating short and long distances is called *operator-product expansion* (OPE). Implicitly or explicitly, OPE is used in almost any perturbative QCD treatment of hadronic processes.

4. LONG-DISTANCE DYNAMICS AND QCD VACUUM

4.1 Vacuum condensates

QCD at short distances does not essentially help in understanding the long-distance dynamics of quarks and gluons. From the short-distance side we only know that the running coupling $\alpha_s(Q)$ increases at low-momentum scales and eventually diverges at $Q \sim \Lambda_{QCD}$ (see Fig. 7). Is the growth of α_s the only dynamical reason for confinement? It is not possible to answer this question remaining within the perturbative QCD framework, because the language of Feynman diagrams with propagators and vertices is not applicable already at $\alpha_s \sim 1$. QCD in nonperturbative regime is currently being studied using other methods, first of all, the lattice simulations. From these studies, there is a growing confidence that long-distance dynamics is closely related to the nontrivial properties of the physical vacuum in QCD.

For a given dynamical system, vacuum is a state with the minimal possible energy. Evidently, in QCD the vacuum state contains no hadrons, because creating any hadron always costs a certain amount of energy. In that sense, QCD vacuum has to be identified with the $\langle 0 |$ state in the correlation function (78). Given that the vacuum state contains no hadrons does not yet mean that it is completely empty. There could be quantum fluctuations of quark and gluon fields with nonvanishing densities. The existence of vacuum fields is manifested, e.g. by *instantons*, special solutions of QCD equations of motion having a form of localized dense gluonic fields (for an introductionary review on instantons see, e.g., [14]). Lattice QCD provides an independent evidence for quark/gluon fields in the vacuum. Without going into further theoretical details, I will rather concentrate on the phenomenology of vacuum fields in QCD. We shall see that properties of hadrons are influenced by the existence of quark and gluon vacuum fluctuations with nonvanishing average densities, the so called *vacuum condensates*.

Formally, in the presence of vacuum fields, the matrix elements of quark and gluon field operators between the initial $|0\rangle$ and final $\langle 0 |$ states are different from zero. The combinations of fields have to obey Lorentz-invariance, colour gauge symmetry and flavour conservation, so that the simplest allowed composite operators are

$$O_3 = \bar{\psi}_{q\,i}\psi_q^i, \ \ O_4 = G_{\mu\nu}^a G^{a\mu\nu}, \ \ O_5 = \bar{\psi}_{q\,i}(\lambda^a)_k^i \sigma_{\mu\nu} G^{a\mu\nu}\psi_q^k,$$
$$O_6 = \left[\bar{\psi}_{q\,i}(\Gamma^a)_k^i \psi_q^k\right]\left[\bar{\psi}_{q'\,j}(\Gamma^a)_l^j \psi_{q'}^l\right], \tag{103}$$

where $\sigma_{\mu\nu} = (i/2)[\gamma_\mu, \gamma_\nu]$ and Γ^a are various combinations of Lorentz- and colour matrices. The indices at O_d reflect their dimension d in GeV units. Furthermore, if the operators are taken at different 4-points, care should be taken of the local gauge invariance. For instance, the quark-antiquark nonlocal matrix element has the following form:

$$\langle 0 \mid \bar{\psi}_q(x)[x,0]\psi_q(0) \mid 0 \rangle, \tag{104}$$

where $[x,0] = \exp\left[ig_s \int_0^1 dv x^\mu A_\mu^a(vx)(\lambda^a/2)\right]$ is the so-called gauge factor. Only the matrix elements with the light quarks $q = u, d, s$ are relevant for the nonperturbative long-distance dynamics. A pair of heavy c (b) quarks can be created in vacuum only at short distances/times of $O(1/2m_c)$ ($O(1/2m_b)$), that is, perturbatively.

Without fully solving QCD, very little could be said about vacuum fields, in particular about their fluctuations at long distances which have typical "wavelengths" of $O(1/\Lambda_{QCD})$. Thus, we are not able

to calculate the matrix element (104) explicitly, as a function of x. It is still possible to investigate the vacuum phenomena in QCD applying certain approximations. One possibility is to study the average local densities. The vacuum average of the product of quark and antiquark fields,

$$\langle 0 \mid \bar{\psi}_{q\,k} \psi_q^k \mid 0 \rangle \equiv \langle \bar{q}q \rangle, \tag{105}$$

corresponds to the $x \to 0$ limit of the matrix element (104). The simplest vacuum density of gluon fields is

$$\langle 0 \mid G_{\mu\nu}^a G^{a\mu\nu} \mid 0 \rangle \equiv \langle GG \rangle. \tag{106}$$

Due to translational invariance, both $\langle \bar{q}q \rangle$ and $\langle GG \rangle$ are independent of the 4-coordinate. These universal parameters are usually called the densities of quark and gluon condensates, respectively. As we shall see in the following subsection, the nonvanishing quark condensate drastically influences the symmetry properties of QCD.

4.2   Chiral symmetry and its violation in QCD

Let us return to the isospin symmetry limit (46) of the QCD Lagrangian:

$$L_{QCD}^{(u=d)} = \overline{\Psi}(iD_\mu\gamma^\mu - \tilde{m})\Psi + L_{glue} + \dots. \tag{107}$$

Since $\tilde{m} \simeq m_u \simeq m_d \ll \Lambda_{QCD}$, a reasonable approximation is to put $\tilde{m} \to 0$, so that u- and d-quark components of the Ψ-doublet become massless.

Each Dirac spinor can be decomposed into the left- and right-handed components,

$$\psi_q = \frac{1+\gamma_5}{2}\psi_q + \frac{1-\gamma_5}{2}\psi_q \equiv \psi_{q\,R} + \psi_{q\,L}, \tag{108}$$

where, by definition, the left-handed (right-handed) quark has an antiparallel (parallel) spin projection on its 3-momentum. Similarly, for the conjugated fields one has:

$$\bar{\psi}_q = \bar{\psi}_q \frac{1-\gamma_5}{2} + \bar{\psi}_q \frac{1+\gamma_5}{2} \equiv \bar{\psi}_{q\,R} + \bar{\psi}_{q\,L}. \tag{109}$$

Rewriting Ψ in terms of the left- and right-handed components we obtain the following decomposition of the Lagrangian (107) in the massless limit:

$$L_{QCD}^{(u=d)} = \overline{\Psi}_R\, iD_\mu\gamma^\mu \Psi_R + \overline{\Psi}_L\, iD_\mu\gamma^\mu \Psi_L + L_{glue} + \dots. \tag{110}$$

The quark-gluon interaction term in $L_{QCD}^{(u=d)}$ is now split into two parts, $g_s\overline{\Psi}_R\gamma_\mu A^{\mu a}(\lambda^a/2)\Psi_R$ and $g_s\overline{\Psi}_L\gamma_\mu A^{\mu a}(\lambda^a/2)\Psi_L$, so that quarks conserve their *chirality* (left- or right-handedness) after emitting /absorbing an arbitrary number of gluons. Importantly, also the interaction of quarks with photons has the same property (take the e.m. interaction (64) and decompose it into L and R parts in the same way as above). In the massless (*chiral*) limit, quarks of left- and right chiralities propagate and interact independently from each other. In fact, it is possible to introduce two independent isospin $SU(2)$ transformations, separately for L and R fields:

$$\begin{aligned}
\Psi_L &\to \Psi'_L = \exp\left(-i\frac{\sigma^a}{2}\omega_L^a\right)\Psi_L, \\
\Psi_R &\to \Psi'_R = \exp\left(-i\frac{\sigma^a}{2}\omega_L^a\right)\Psi_R.
\end{aligned} \tag{111}$$

Restoring the mass in $L_{QCD}^{(u=d)}$ leads to the violation of chiral symmetry. The Lagrangian mass term can be represented as an effective transition between left- and right-handed quarks:

$$\tilde{m}\overline{\Psi}\Psi = \tilde{m}\left(\overline{\Psi}_L\Psi_R + \overline{\Psi}_R\Psi_L\right). \tag{112}$$
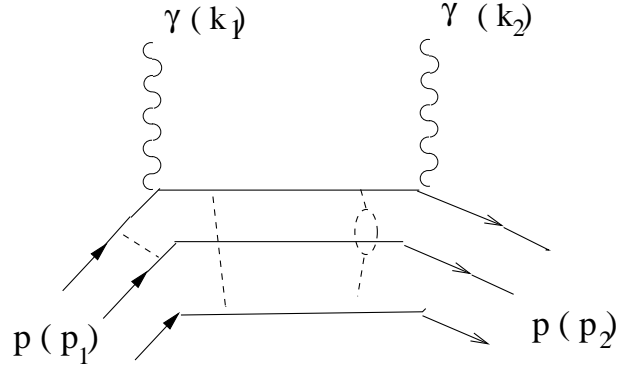
Fig. 18: *One of the diagrams describing the photon-proton scattering. The second diagram is obtained by interchanging the photon lines.*

Having in mind the smallness of the u, d-quark masses, one naturally expects that an approximate chiral symmetry manifests itself in the observable properties of hadrons. In reality, the symmetry is violated quite substantially, as the two following examples demonstrate.

The first one is a real hadronic process: the photon scattering on a polarized (e.g. left-handed) proton. One of the diagrams is shown in Fig. (18). This process is a very complicated mixture of quark-photon and quark-gluon interactions at long distances, determined by the quark structure of the proton. Importantly, all these interactions obey an approximate chiral symmetry at the Lagrangian level. Hence, the amplitude of the proton-chirality flip is expected to be very small, $O(m_{u,d}/\Lambda_{QCD}) \sim 1\%$ of the total scattering amplitude. To check this conjecture, let me consider the case when the initial photon energy is much smaller than the proton mass. In this case, it is possible to approximate the proton with a point-like particle. The $\gamma p \to \gamma p$ amplitude is then simply obtained from the $\gamma e \to \gamma e$ amplitude in QED (Compton effect), replacing the electron spinors and propagators by the proton ones:

$$A(\gamma p \to \gamma p) \simeq e^2 \bar{u}(p_2) \left[\gamma_\alpha \frac{(p_1 + k_1)_\mu \gamma^\mu + m_p}{(p_1 + k_1)^2 - m_p^2} \gamma_\beta + \gamma_\beta \frac{(p_1 - k_2)_\mu \gamma^\mu + m_p}{(p_1 - k_2)^2 - m_p^2} \gamma_\alpha \right] u_L(p_1) \epsilon_2^\alpha \epsilon_1^\beta, \quad (113)$$

where $\epsilon_{1,2}$ are the polarization vectors of the initial and final photons with the 4-momenta k_1 and k_2, respectively. Without even completing the calculation, we notice that the $\sim m_p$ terms in the amplitude flip the initial proton chirality $L \to R$, whereas the $\sim \gamma_\mu$ terms preserve chirality. Importantly, the contributions of both types are of the same order, determined by the scale m_p, indicating that chiral symmetry for the photon-proton scattering is broken at 100% level.

To present the second example of the chiral symmetry violation, I start from the correlation function

$$\Pi_{\mu\nu} = i \int d^4x e^{iqx} \langle 0|T\{j_\mu(x)j_\nu(0)\}|0\rangle = (-g_{\mu\nu}q^2 + q_\mu q_\nu)\Pi(q^2), \quad (114)$$

very similar to the one introduced in Lecture 3, but containing a slightly different quark current:

$$j_\mu = \frac{1}{2}(\bar{\psi}_u \gamma_\mu \psi_u - \bar{\psi}_d \gamma_\mu \psi_d), \quad (115)$$

which produces the $I = 1$ and $J^P = 1^-$ quark-antiquark states. Note that this current is conserved, $\partial_\mu j^\mu = 0$, even if $m_{u,d} \neq 0$. We then follow the same derivation as in Lecture 3 and obtain the

dispersion relation (89) for $\Pi(q^2)$. The only change is in the imaginary part (90), where now only the states with $I = 1$ contribute to the total cross section (ρ meson and its radial excitations, the two-pion state and other states with an even number of pions), so that the ratio $R(s)$ has to be replaced by

$$R^{(I=1)}(s) = \frac{\sigma_{tot}(e^+e^- \to h(I = 1))}{\sigma(e^+e^- \to \mu^+\mu^-)} \, . \tag{116}$$

In parallel, we consider the correlation function

$$\Pi^5_{\mu\nu} = i \int d^4x e^{iqx} \langle 0|T\{j_{\mu5}(x)j_{\nu5}(0)\}|0\rangle \tag{117}$$

of two axial-vector currents with $I = 1$:

$$j_{\mu5} = \frac{1}{\sqrt{2}}(\bar{\psi}_u\gamma_\mu\gamma_5\psi_u - \bar{\psi}_d\gamma_\mu\gamma_5\psi_d) \, . \tag{118}$$

This current is conserved only in the chiral symmetry ($m_{u,d} = 0$) limit:

$$\partial^\mu j_{\mu5} = \frac{1}{\sqrt{2}}(2m_u\bar{\psi}_u\gamma_5\psi_u - 2m_d\bar{\psi}_d\gamma_5\psi_d) \, . \tag{119}$$

Decomposing the correlation function (117) in two tensor structures:

$$\Pi^5_{\mu\nu}(q) = -g_{\mu\nu}\Pi'_5(q^2) + q_\mu q_\nu\Pi_5(q^2) \, , \tag{120}$$

we notice that in the chiral limit there is only one independent invariant amplitude:

$$\Pi_5(q^2) = \frac{\Pi'_5(q^2)}{q^2} \, . \tag{121}$$

The dispersion relation for Π_5 has the same form as (89):

$$\Pi_5(q^2) = \frac{1}{\pi}\int\limits_{s^5_{min}}^{\infty} ds\frac{\text{Im}\Pi_5(s)}{s - q^2 - i\delta} \, , \tag{122}$$

where s^5_{min} is the corresponding threshold. In order to determine the imaginary part via relation similar to (90), we introduce a slightly artificial cross section $\sigma_{tot}(e^+e^- \to Z^A \to h(I = 1))$ of hadron production mediated by Z boson coupled to the axial-vector current. Then,

$$\text{Im}\Pi_5(s) = \frac{1}{12\pi}R^{(I=1)}_5(s) \, , \tag{123}$$

where

$$R^{(I=1)}_5(s) = \frac{\sigma^{(e^+e^- \to Z^A \to h(I=1))}_{tot}(s)}{\sigma^{(e^+e^- \to Z^A \to \mu^+\mu^-)}(s)} \, . \tag{124}$$

Both $\Pi(q^2)$ and $\Pi_5(q^2)$ can be calculated at large $|q^2|$ from the same 2-point quark-loop diagrams shown in Fig. 14. In the chiral limit, the only difference is in two extra γ_5 matrices present in $\Pi^5_{\mu\nu}$. Hence, in perturbative QCD

$$\Pi_5(q^2) = \Pi(q^2) \, , \tag{125}$$

at any order in α_s. This equation is trivial for the leading-order loop diagrams (Fig. 14a). Using Dirac algebra, it is easy to check that the extra γ_5 matrices cancel each other ($\gamma_5^2 = 1$) in the absence of masses in the propagators. Furthermore, each gluon line inserted in the loop brings two more γ-matrices which do not influence that cancellation.
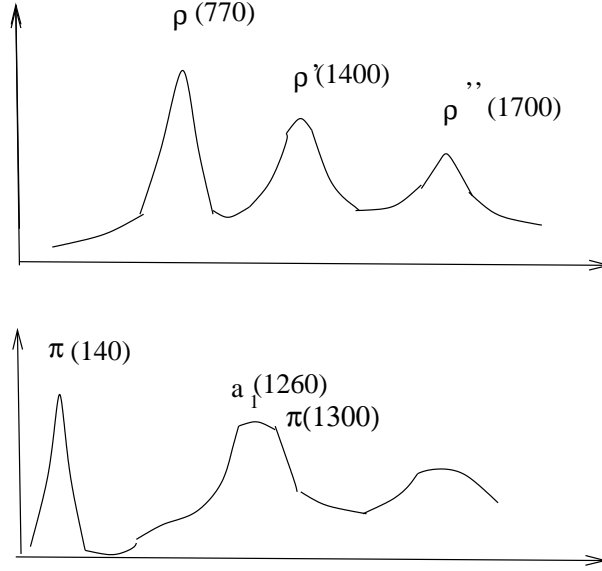
Fig. 19: *A schematic pattern of the resonances produced by the vector (above) and axial-vector (below) quark currents with $I = 1$.*

From (125) follows the equation of two dispersion relations (89) and (122). To keep the dispersion integrals convergent, we differentiate them n times at a certain $q^2 < 0$. The result is:

$$\int\limits_{s_{min}}^{\infty} ds \frac{R_5(s)}{(s - q^2)^n} = \int\limits_{s_{min}}^{\infty} ds \frac{R(s)}{(s - q^2)^n} \,. \tag{126}$$

Note that even in the presence of quark masses the corrections to (125) and to (126) are very small, $O(m_{u,d}^2)$. If q^2 is not very large, $|q^2| \sim 1\,\mathrm{GeV}^2$, the integrals in (126) are dominated by the contributions of the low-mass hadronic states to the corresponding $e^+ e^- \to h$ cross sections. In the case of vector current, the states are ρ-meson and its radial excitations. Hence, $R(s)$ represents a resonance curve with the peaks located at $s = m_\rho^2$, $m_{\rho'}^2$ etc. (see Fig. 19). The validity of (126) at arbitrary (but large) $q^2 < 0$ implies that also $R_5(s) \simeq R(s)$. We then expect the spectrum of resonances generated by the axial-vector current to resemble, in gross features, the ρ-spectrum. However, experimental data [4] reveal a completely different picture. The lowest resonances in the axial-vector channel are the pion with $J^P = 0^-$, the axial meson $a_1(1260)$ and the radial excitation $\pi(1300)$. Summarizing, there is a clear evidence, based on the observed properties of hadrons, that chiral symmetry in QCD is violated much stronger than it is expected from L_{QCD}.

An additional source of the chiral symmetry violation is provided by the quark condensate. Decomposing the quark and antiquark fields in (105) in the left-handed and right-handed components,

$$\langle 0 | \bar{\psi}_{q\,i} \psi_q^i | 0 \rangle = \langle 0 | (\bar{\psi}_{qR} + \bar{\psi}_{qL})(\psi_{qR} + \psi_{qL}) | 0 \rangle = \langle 0 | \bar{\psi}_{qR} \psi_{qL} + \bar{\psi}_{qL} \psi_{qR}) | 0 \rangle \neq 0 \,, \tag{127}$$

we realize that condensate causes vacuum transitions between quarks of different chiralities. Hence, in QCD one encounters a *spontaneous broken* chiral symmetry, a specific situation when the interaction (in this case L_{QCD}) obeys the symmetry (up to the small $O(m_{u,d})$ corrections), whereas the lowest-energy state (QCD vacuum) violates it [10]. We conclude that in order to correctly reproduce the properties of hadrons and hadronic amplitudes (e.g., correlation functions), one has to take into account the vacuum fields, in particular, the quark condensate.

---

[10]That is quite similar to the electroweak sector of the Standard Model [1], where the electroweak gauge symmetry is spontaneously broken by the nonvanishing vacuum average of the Higgs field.
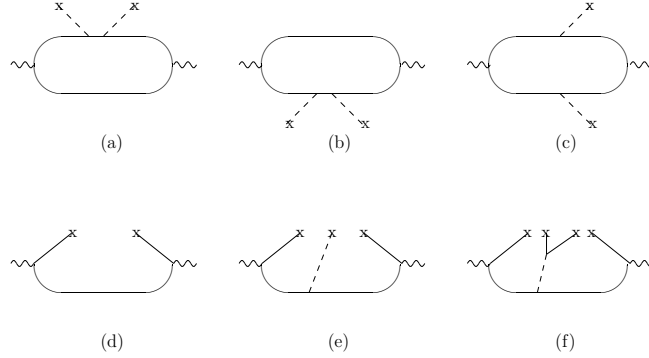
Fig. 20: *Diagrams used to calculate condensate contributions to the correlation functions of two quark currents. Lines with crosses denote vacuum fields.*

4.3 Condensate contributions to correlation functions

Let us return to the correlation functions (114) and (117), restoring nonzero u and d quark masses, that is, working with full QCD. The vacuum quark-gluon fields generate new contributions to Π or Π_5. In addition to the perturbative loop diagrams in Fig. 14, there are diagrams shown in Fig. 20, where gluons, quarks and antiquarks penetrate to long distances, being absorbed and emitted by vacuum fluctuations. The vacuum fields have characteristic momenta of $O(\Lambda_{QCD})$. Therefore, if the momentum scale in the correlator is large, $Q = \sqrt{-q^2} \gg \Lambda_{QCD}$, one can approximate the vacuum state by a set of constant fields. In other words, the virtual quark propagating at short distances/times between the points x and 0, cannot "resolve" the long-distance fluctuations of vacuum fields and percepts them in a form of averaged static fields. This approximation makes the calculation of diagrams in Fig. 20 straightforward. In addition to Feynman rules of perturbative QCD for virtual quarks and gluons, one has to form all possible combinations (103) of vacuum fields and replace them by the corresponding condensate densities, so that the 4-momenta of the crossed lines on these diagrams are neglected. For example, the product of quark and antiquark vacuum fields in Fig. 20 d has to be replaced by $\langle \bar{q}q \rangle$. More details on these calculations can be found, e.g., in the review [15]. The result for the vector-current correlator has the following schematic form:

$$\Pi(q^2) = \Pi^{pert}(q^2) + \sum_{d=3,4,\dots} C_d(q^2)\langle 0|O_d|0\rangle \,, \tag{128}$$

where the first term on r.h.s. corresponds to the perturbative diagrams in Fig. 14, whereas the sum contains the contributions of vacuum condensates with dimensions d obtained from the diagrams in Fig. 20. To compensate the growing dimension of the operators O_d, the coefficients C_d contain increasing powers of $1/Q$. Thus, the condensate contributions die away at $Q \to \infty$ and do not alter the perturbative asymptotics of the correlator given by $\Pi^{pert}(q^2)$. Furthermore, as soon as we work at relatively large $Q \gg \Lambda_{QCD}$, it is possible to retain only a few first terms in the sum , that is, neglect diagrams with more than 3-4 vacuum fields emitted from the virtual quarks in the correlation function.

For the axial-vector correlation function $\Pi_5(q^2)$ one obtains an expression similar to (128) with the same perturbative part (up to very small corrections of $O(m_{u,d}^2)$), but with different coefficients C_d at certain condensate terms. The most important deviation from the vector-current case is in the value and sign of C_6, i.e., in the 4-quark condensate terms. Thus, addition of condensate effects leads to an explicit violation of (125). It is then not surprising that hadron resonances contributing to $R(s)$ and $R_5(s)$ in (126) are different.

Furthermore, the method of correlation functions allows to reproduce an important relation for the pion mass, explaining the smallness of m_π. Note that from the point of view of naive quark model π and ρ mesons differ only by orientations of quark spins. Why is then $m_\pi \ll m_\rho$ and, moreover, $m_\pi < \Lambda_{QCD}$? We consider the correlation function similar to (117), but for simplicity, containing charged axial currents:

$$\Pi^5_{\mu\nu} = i \int d^4 x e^{iqx} \langle 0|T\{j_{\mu5}(x)j^\dagger_{\nu5}(0)\}|0\rangle = -g_{\mu\nu}\Pi'_5(q^2) + q_\mu q_\nu \Pi_5(q^2), \tag{129}$$

where $j_{\mu5} = \bar{u}\gamma_\mu\gamma_5 d$. This current is the part of the Standard Model weak current (67), responsible for $u \to d$ transition, e.g. the $\pi \to \mu\nu_\mu$ decay. The hadronic matrix element which determines this decay,

$$\langle 0|\bar{u}\gamma_\mu\gamma_5 d|\pi^+(q)\rangle = iq_\mu f_\pi, \tag{130}$$

is parameterized via the pion decay constant f_π which plays an essential role in our analysis. It is convenient to multiply (129) by $q_\mu q_\nu/q^2$, forming a combination of invariant amplitudes:

$$-\frac{q^\mu q^\nu}{q^2}\Pi^5_{\mu\nu} = \Pi'_5(q^2) - q^2\Pi_5(q^2) \equiv \tilde{\Pi}_5(q^2).$$

Note that $\tilde{\Pi}_5 = 0$ at $m_{u,d} = 0$ and, in particular, the perturbative part of $\tilde{\Pi}_5$ vanishes as $O(m^2_{u,d})$. Concerning nonperturbative part, the only first-order in $m_{u,d}$ contribution is given by the quark condensate diagram in Fig. 20d

$$\tilde{\Pi}_5(q^2) = -\frac{(m_u + m_d)(\langle \bar{u}u\rangle + \langle \bar{d}d\rangle)}{q^2} + O(m^2_{u,d}). \tag{131}$$

To proceed, we use for $\tilde{\Pi}_5$ the dispersion relation of the type (122). To obtain the imaginary part, one has to return to the unitarity relation (75), identifying $|i\rangle$ with $|0\rangle$ and T_{ii} with the correlation function. The result is:

$$2\mathrm{Im}\tilde{\Pi}_5(s) = -\frac{q^\mu q^\nu}{q^2}\sum_{h_n}\langle 0|j_{\mu5}|h_n\rangle\langle h_n|j^\dagger_{\nu5}(q)|0\rangle. \tag{132}$$

Importantly, only pseudoscalar states contribute to the above sum, because the matrix elements for the axial-vector mesons a_1 and its excitations vanish, being proportional to the transverse polarization vectors of these mesons:

$$q^\mu\langle 0|j_{\mu5}|a_1\rangle \sim q^\mu\epsilon^{a_1}_\mu = 0.$$

Using (132) and the definition (130) we obtain the following expression for the dispersion relation:

$$\begin{aligned}
\tilde{\Pi}_5(q^2) &= \frac{1}{2\pi}\int_{m^2_\pi}^\infty \frac{ds}{s - q^2 - i\delta}\left\{-\frac{q^\mu q^\nu}{q^2}(f_\pi q_\mu)(f_\pi q_\nu)\int\frac{d^3 p_\pi(2\pi)}{2E_\pi}\delta^{(4)}(p_\pi - q)\right\}_{q^2=s} + \dots \\
&= \int_{m^2_\pi}^\infty \frac{ds}{s - q^2 - i\delta}\left\{-f^2_\pi s\delta(s - m^2_\pi)\right\} + \dots,
\end{aligned} \tag{133}$$

where the one-pion state contribution is shown explicitly (with $p^2_\pi = m^2_\pi$) including the phase space proportional to δ-function. Ellipses denote excited pions and multiparticle states with the same quantum numbers. Integrating out δ-function and substituting (131) in l.h.s. we obtain

$$-\frac{(m_u + m_d)(\langle \bar{u}u\rangle + \langle \bar{d}d\rangle)}{q^2} + O(m^2_{u,d}) = -\frac{f^2_\pi m^2_\pi}{m^2_\pi - q^2} - \sum_{\pi'}\frac{f^2_{\pi'}m^2_{\pi'}}{m^2_{\pi'} - q^2}, \tag{134}$$

where the sum over higher states is also shown schematically. To fulfil this equation at large q^2 one has to demand that $m^2_\pi \sim m_u + m_d$. Simultaneously, the decay constants of excited states have to obey:

$f_{\pi'} \sim m_u + m_d$, otherwise the q^2 asymptotics of l.h.s and r.h.s. in (134) is different at $O(m_{u,d})$. We then reproduce the well known Gell-Mann-Oakes-Renner relation

$$- (m_u + m_d)(\langle \bar{u}u \rangle + \langle \bar{d}d \rangle) + O(m_{u,d}^2) = f_\pi^2 m_\pi^2 \,. \tag{135}$$

This relation reflects the special nature of pion in QCD. The anomalously small pion mass is not accidental and is closely related to the spontaneous chiral symmetry breaking via condensate. If a symmetry in quantum field theory is broken spontaneously, there should be massless states (Nambu-Goldstone particles), one per each degree of freedom of broken symmetry. The three pions, π^+, π^-, π^0 play a role of massless Nambu-Goldstone particles in QCD. In other words, due to the specific structure of QCD vacuum fields, the amount of energy needed to produce a pion state tends to zero. The fact that pions still have small nonvanishing masses is due to the explicit violation of chiral symmetry via u, d quark masses.

How large is the quark condensate density? Using $m_{\pi^\pm} \simeq 140$ MeV, $f_\pi = 131$ MeV [4] and taking the u, d quark mass values from (31), renormalizing them at $Q = 1$ GeV, one obtains from (135), typically,

$$\langle \bar{q}q \rangle (\mu = 1 GeV) \simeq (-240 \pm 10 \text{ MeV})^3 \,, \tag{136}$$

where we assume isospin symmetry for the condensates $\langle \bar{q}q \rangle \simeq \langle \bar{u}u \rangle \simeq \langle \bar{d}d \rangle$. Not surprisingly, the estimated value is in the ballpark of Λ_{QCD} ! Being not a measurable physical quantity, the condensate density is a scale-dependent parameter. Since r.h.s. of (135) is determined by hadronic parameters f_π, m_π, which are both scale-independent, the running of the quark condensate should compensate the running of the quark mass given in (37), that is:

$$\langle \bar{q}q \rangle (Q) = \langle \bar{q}q \rangle (Q_0) \left(\frac{\alpha_s(Q)}{\alpha_s(Q_0)} \right)^{-\gamma_0/\beta_0} \,. \tag{137}$$

4.4 Gluon condensate

The gluon condensate density is another important characteristics of nonperturbative QCD. This parameter cannot be easily estimated from correlation functions with light quarks, because the latter are dominated by quark condensates. A very useful object, sensitive to the gluon condensate is the correlation function of c-quark currents:

$$\Pi_{\mu\nu}^c = i \int d^4 x e^{iqx} \langle 0|T\{j_\mu^c(x)j_\nu^c(0)\}|0 \rangle = (-g_{\mu\nu}q^2 + q_\mu q_\nu)\Pi^c(q^2) \,, \tag{138}$$

where $j_\mu^c = \bar{c}\gamma_\mu c$ is the c-quark part of the quark e.m. current j_μ^{em}. Following the same derivation as in Lecture 3, we write down the dispersion relation for $\Pi^c(q^2)$ relating $\text{Im}\Pi^c(s)$ with the ratio $R_c(s)$ defined as:

$$R_c = \frac{\sigma(e^+e^- \to charm)}{\sigma(e^+e^- \to \mu^+\mu^-)} \,, \tag{139}$$

where the cross section $\sigma(e^+e^- \to charm)$ includes hadronic states with $\bar{c}c$ content produced in e^+e^-: charmonium resonances ($J/\psi, \psi', ...$), pairs of charmed hadrons etc. In addition to the perturbative c-quark loop diagrams in Fig 14, one has to include also the contribution of the diagrams shown in Fig 20a,b,c, with c quarks emitting vacuum gluons. (Remember that nonperturbative quark condensate for the heavy c quark is absent.) The resulting relation has the following form:

$$\int\limits_{m_\psi^2}^\infty \frac{ds}{s - q^2} R_c(s) = \Pi^{pert}(q^2, m_c^2, \alpha_s) + \frac{\alpha_s}{\pi} \langle GG \rangle f_c(q^2, m_c^2) \,, \tag{140}$$

where m_ψ is the mass of the lowest J/ψ state in this channel. The function Π^{pert} evaluated from the massive c-quark loop diagrams has a more complicated form than in the massless case. The function f_c

is the calculable short-distance part of the diagrams in Fig. 20a,b,c. To achieve a better convergence at $s \to \infty$, the dispersion relation is usually differentiated n times. Note that in this case the point $q^2 = 0$ is also accessible: c quarks are still highly virtual at $q^2 = 0$ because the long-distance region starts at $q^2 \sim 4m_c^2$. The set of power moments obtained from (140) with $O(\alpha_s^2)$ accuracy has a form

$$\int\limits_{m_\psi^2}^{\infty} \frac{ds}{s^{n+1}} R^c(s) = \frac{3Q_c^2}{(4m_c^2)^n} r_n \left[1 + \alpha_s(m_c)a_n + (\alpha_s(m_c))^2 a_n' + b_n \frac{\langle \frac{\alpha_s}{\pi} GG \rangle}{(4m_c^2)^2} \right], \qquad (141)$$

with calculable coefficients r_n, a_n, a_n', b_n. The natural scale for α_s in the perturbative loops is in this case the virtuality $Q \sim m_c$. The moments (141) are used to extract the gluon condensate density and, simultaneously the c quark mass, employing the experimental data on $R_c(s)$ on l.h.s. The estimate of the condensate density obtained first in [17] is:

$$\frac{\alpha_s}{\pi} \langle GG \rangle = (330 \text{ MeV})^4 \pm 50\%, \qquad (142)$$

again within the range of Λ_{QCD}. The value of the gluon condensate density is usually given multiplied by α_s for convenience, because this product is scale-independent.

5. RELATING QUARKS AND HADRONS: QCD SUM RULES

5.1 Introducing the method

The relation (141) obtained first in [16] is a well known example of a *QCD sum rule*. The method developed by Shifman, Vainshtein and Zakharov [17] employs quark-current correlation functions calculating them in the spacelike region, including perturbative and condensate contributions. Consider for example the correlation function (114), with the result of QCD calculation having the form (128). Note that in the latter expression short- and long-distance effects are separated. The perturbative part $\Pi^{pert}(q^2)$ and the coefficients $C_d(q^2)$ take into account short-distance quark-gluon interactions with characteristic momenta larger than the scale Q. Both Π^{pert} and C_d are *process-dependent*, i.e., depend on the choice of the currents. On the other hand, the condensate densities absorb, in an averaged way, the long-distance interactions with momenta less than Q and are process-independent. The universality of condensates allows to calculate correlation functions in different channels without introducing new inputs, in an almost model-independent way [11]. To obtain the sum rule, the QCD result for the correlation function is matched, via dispersion relation, to the sum over hadronic contributions (the integral over hadronic cross section).

A twofold use of the sum rule relations is possible. Firstly, using experimental data one saturates the hadronic sum in the dispersion integral and extracts the universal QCD parameters: quark masses, α_s, condensate densities. One example is the $c\bar{c}$ sum rule (141) discussed above. Secondly, having fixed QCD parameters, one calculates, with a certain accuracy, the masses and decay amplitudes of the lowest hadrons entering the dispersion integral. The relation (135) obtained from the sum rule (134) can serve as an example. Note that (134) is unique, because all states in the hadronic sum except the pion and all QCD terms except the quark condensate are absent at $O(m_{u,d})$.

5.2 The ρ-meson decay constant

To demonstrate in more detail how the method works [12], let me outline the calculation of the ρ-meson decay constant from the correlation function (114). The dispersion relation for $\Pi_{\mu\nu}$ can be written in the

---

[11]The expansions similar to (128) represent another example of OPE in QCD (see Lecture 3.3), when a product of two currents is expanded in a set of local operators O_d. The perturbative part in this case is interpreted as a unit operator with zero dimension.

[12]reviews can be found e.g., in [15],[18].

following form:

$$\Pi_{\mu\nu}(q) = \frac{1}{2\pi} \int\limits_{s_{min}}^{\infty} \frac{ds}{s - q^2 - i\delta} \left\{ \sum_{h_n} \langle 0|j_\mu|h_n\rangle\langle h_n|j_\nu(q)|0\rangle \right\}$$

$$= \int\limits_{s_{min}}^{\infty} \frac{ds}{s - q^2 - i\delta} \left\{ \left[\frac{f_\rho^2}{2}\delta(s - m_\rho^2) + \rho^h(s) \right] (-g_{\mu\nu}q^2 + q_\mu q_\nu) \right\}_{q^2=s}, \qquad (143)$$

where the ρ-meson contribution ($h_n = \rho^0$) is isolated from the sum and the hadronic matrix element is substituted:

$$\langle 0|j_\mu|\rho^0\rangle = \frac{f_\rho}{\sqrt{2}}m_\rho\epsilon_\mu^{(\rho)}, \qquad (144)$$

determined by the ρ decay constant f_ρ. The integrand $\rho^h(s)$ (*spectral density*) includes the sum over excited and multihadron states. We take into account the experimental fact that the ρ resonance strongly dominates in the low-energy region $2m_\pi < \sqrt{s} < 1$ GeV, so that $\rho^h(s)$ practically starts from some threshold value $s_0 \sim 1$ GeV. Switching to the invariant amplitude $\Pi(q^2)$ and using the result (128) of QCD calculation, one obtains from (143) the desired relation, a prototype of QCD sum rule:

$$\frac{f_\rho^2}{2(m_\rho^2 - q^2)} + \int\limits_{s_0}^{\infty} \frac{ds\,\rho^h(s)}{s - q^2 - i\delta} = \Pi^{pert}(q^2) + \sum_{d=3,4,...} C^d(q^2)\langle 0|O_d|0\rangle, \qquad (145)$$

which is valid at sufficiently large $|q^2|$. To proceed, one applies to both sides of this equation the *Borel transformation* defined as:

$$\hat{B}_{M^2}\Pi(q^2) = \lim_{\substack{-q^2,n\to\infty \\ -q^2/n=M^2}} \frac{(-q^2)^{(n+1)}}{n!}\left(\frac{d}{dq^2}\right)^n \Pi(q^2) \equiv \Pi(M^2). \qquad (146)$$

This transformation deserves a clarifying comment. Differentiating $\Pi(q^2)$ many times in q^2 means, one is effectively approaching the long-distance region. Indeed, with an infinite amount of derivatives the function $\Pi(q^2)$ is defined at any q^2, including $q^2 > 0$. The $q^2 \to -\infty$ limit works in the opposite direction: one penetrates into the deep spacelike asymptotics. Combining the two transformations in (146) at $M^2 = -q^2/n$, one fixes the virtuality scale at $O(M)$. Using the school-textbook definition of the exponent: $e^x = \lim_{n\to\infty}(1 + x/n)^n$, it is an easy exercise to prove that

$$\hat{B}_{M^2}\left\{\frac{1}{m_h^2 - q^2}\right\} = e^{-m_h^2/M^2}. \qquad (147)$$

As a result, Borel transformation exponentially suppresses the integral over $\rho^h(s)$ in (145) with respect to the ρ-meson term. Furthermore, after applying $\hat{B}$ to r.h.s. of (145) the coefficients $C_d(M)$ contain powers of $1/M^2$. Hence, at large M^2 it is possible to retain only a few low-dimension condensates in the sum, e.g., at $M^2 \sim 1$ GeV^2 a reasonable approximation is to neglect all operators with $d > 6$. The explicit form of the QCD sum rule (145) after Borel transformation is [17]:

$$\frac{f_\rho^2}{2}e^{-m_\rho^2/M^2} + \int\limits_{s_0}^{\infty} ds\,\rho^h(s)e^{-s/M^2}$$

$$= \frac{M^2}{2}\left[\frac{1}{4\pi^2}\left(1 + \frac{\alpha_s(M)}{\pi}\right) + \frac{(m_u+m_d)\langle\bar{q}q\rangle}{M^4} + \frac{1}{12}\frac{\langle\frac{\alpha_s}{\pi}G_{\mu\nu}^a G^{a\mu\nu}\rangle}{M^4} - \frac{112\pi}{81}\frac{\alpha_s\langle\bar{q}q\rangle^2}{M^6}\right]. \qquad (148)$$

In obtaining the above relation, the four-quark vacuum densities are factorized into a product of quark condensates. The quark-gluon condensate has very small coefficient and is neglected. The running
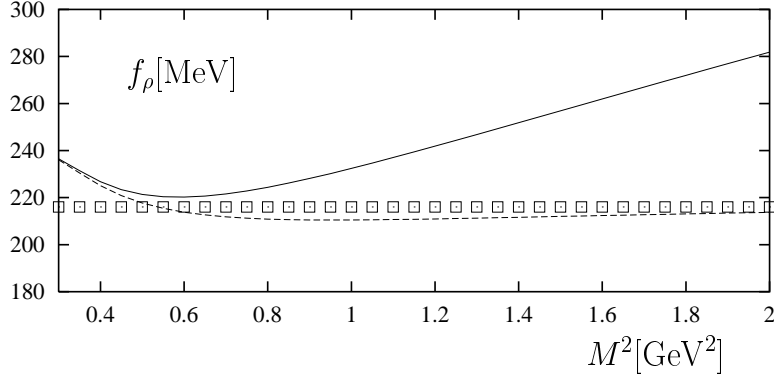
Fig. 21: *The ρ meson decay constant calculated from the sum rule (148) neglecting all excited and continuum states (solid), as a function of the Borel parameter, in comparison with the experimental value (boxes). The dashed curve corresponds to an improved calculation , where the sum over excited and continuum states is estimated using quark-hadron duality with a threshold $s_0^\rho = 1.7$ GeV^2.*

coupling α_s is taken at the scale M i.e., at the characteristic virtuality of the loop diagrams after Borel transformation.

Importantly, there exists a SVZ region [17] of intermediate M^2 where the ρ meson contribution alone saturates the l.h.s. of the sum rule (148). To illustrate this statement numerically, in Fig. 21 the experimentally measured f_ρ (obtained from the $\rho^0 \to e^+ e^-$ width) is compared with the same hadronic parameter calculated from the sum rule (148) where all contributions of excited and continuum states are neglected. One indeed observes a good agreement in the region $M^2 \sim 1$ GeV^2.

An important step to improve the sum rule (148) is to use the *quark-hadron duality* approximation. The perturbative contribution to the correlation function (the sum of Fig. 14 diagrams) is represented in the form of a dispersion integral splitted into two parts:

$$\Pi^{pert}(q^2) = \int\limits_0^{s_0} \frac{ds\, \rho^{pert}(s)}{s - q^2 - i\delta} + \int\limits_{s_0}^\infty \frac{ds\, \rho^{pert}(s)}{s - q^2 - i\delta} \,. \tag{149}$$

The integral over the spectral function $\rho^h(s)$ in (145) is approximated by the second integral over the perturbative spectral density $\rho^{pert}(s)$ in (149). The latter integral is then subtracted from both parts of (145). Correspondingly (148) is modified: the l.h.s. contains only the ρ term, and, on the r.h.s., the perturbative contribution has to be multiplied by a factor $(1 - e^{-s_0/M^2})$. The numerical result obtained from the duality-improved sum rule (148) is also shown in Fig. 21. The agreement between the sum rule prediction and experiment is impressive:

$$f_\rho^{(QCDSR)} = 213 \text{ MeV} \pm (10 - 15)\% \tag{150}$$

whereas $f_\rho^{exp} = 216 \pm 5$ MeV [4]. The estimated theoretical uncertainty quoted in (150) is typical for QCD sum rules, reflecting the approximate nature of this method. So far we only reproduced f_ρ, using the experimental value of m_ρ. In principle, it is possible to go one step further and estimate also the ρ-mass from the sum rule . Furthermore, a very similar sum-rule analysis for the correlation function of axial currents (129) (the invariant amplitude Π_5) successfully reproduces the value of f_π (see Fig. 22).
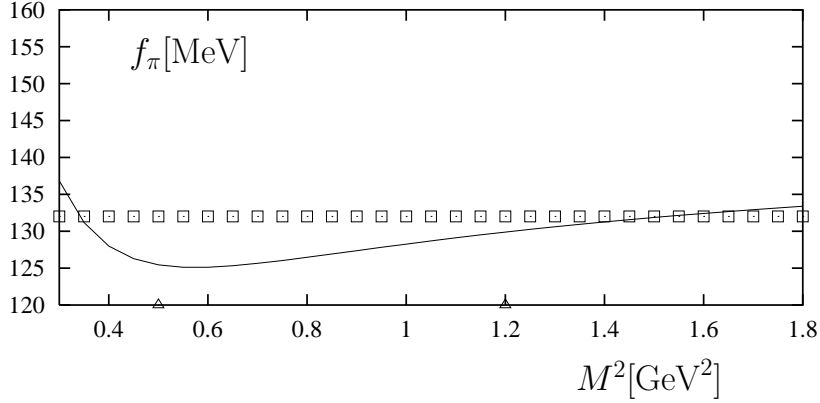
Fig. 22: *The π meson decay constant calculated from QCD sum rule [17] for the correlation function of axial-vector currents (solid line), in comparison with the experimental value (boxes). The quark-hadron duality threshold is fitted simultaneously as $s_0^\rho = 0.7$ GeV^2. The uncertainty of about 10-15% has to be added to the theoretical curve.*

5.3 Baryons

It is possible to extend the method of QCD sum rules to baryons [19, 20]. The idea is to construct special quark currents with baryon quantum numbers which can serve as a source of baryon production/annihilation from/to QCD vacuum. In reality, such currents hardly exist [13], but they are allowed in QCD if colour-neutrality is obeyed. A well known example is the Ioffe current with the nucleon quantum numbers (i.e., spin 1/2):

$$J^N(x) = \epsilon_{abc}(u^{aT}(x)\hat{C}\gamma_\mu u^b(x))\gamma_5\gamma^\mu d^c(x) \,, \tag{151}$$

where a, b, c are color indices, $\hat{C} = \gamma_2\gamma_0$ is the charge conjugation matrix and, for definiteness, the proton flavour content is chosen. As a next step, one constructs a correlation function

$$\Pi_N(q) = i \int d^4x e^{iqx} \langle 0|T\{J^N(x)\bar{J}^N(0)\}|0\rangle \,. \tag{152}$$

The corresponding diagrams are shown in Fig. 23, including perturbative loops and vacuum condensates. They look quite different from the quark-antiquark loops, but differences concern the short-distance parts of the diagrams. The universality of condensates allows one to calculate $\Pi_N(q)$ without introducing new input parameters. The hadronic contribution contains a total sum over states produced and annihilated by the current J^N, starting from the lowest possible state, the nucleon:

$$\Pi_N(q) = \frac{\langle 0|J^N|N\rangle\langle 0|\bar{J}^N|N\rangle}{m_N^2 - q^2} + \{\text{excited resonances, multiparticle states}\} \,. \tag{153}$$

The derivation of the QCD sum rule is done along the same lines as in the previous subsection. Omitting the details, let me only mention that from this sum rule an approximate formula for the nucleon mass is obtained,

$$m_N \simeq [-(2.0)(2\pi)^2\langle 0|\bar{q}q|0\rangle(\mu = 1\text{GeV})]^{1/3} \,, \tag{154}$$

---

[13]In models of Grand Unification predicting proton decay via intermediate superheavy particles, the currents we are discussing are realized effectively in a form of localized 3-quark operators annihilating the proton.
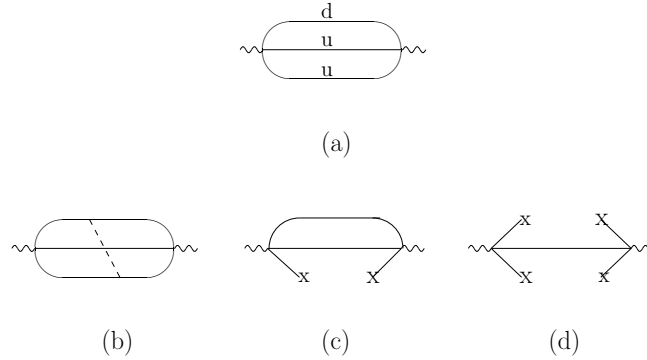
Fig. 23: *Some of the diagrams contributing to the correlation function of two baryon currents: (a) the lowest-order tree-quark two-loop diagram; (b) the $O(\alpha_s)$ correction, (c),(d) -quark condensate diagrams.*

relating it to the quark-condensate density. In fact, the quark masses $m_{u,d}$ themselves generate very small corrections to this relation and are neglected. Thus, QCD sum rules provide an answer to the question that was raised in Lecture 1: almost 99% of the baryonic mass in the Universe are due to vacuum condensates.

5.4 Quark mass determination

As already mentioned, the sum rule (141) can be used to extract the c-quark mass. Here, the role of Borel transformation is played by a simple differentiation at $q^2 = 0$, which turns out to be more useful. At low n, the moments (141) are especially convenient for m_c determination because the gluon condensate effects are small. Replacing $c \to b$, $\psi \to \Upsilon$, etc., one obtains analogous sum rule relations for b quark, where gluon condensate is much less important, being suppressed by m_b^{-4}. Recent analysis [21] of these sum rules yields $m_c(m_c) = 1.304 \pm 0.027$ GeV, $m_b(m_b) = 4.209 \pm 0.05$ GeV. Another subset of charmonium sum rules (higher moments at fixed large $q^2 < 0$) was recently employed in [22], with a prediction for m_c in agreement with the above.

The heavy-quark mass determination using sum rules is also done in a different way, employing the large n moments (141) which are less sensitive to the cross-section above the open flavour threshold. These moments, however, demand a careful treatment of Coulomb interactions between heavy quark and antiquark in the perturbative diagrams. Remember that one-gluon exchange yields Coulomb potential. Close to the threshold of heavy quark-pair production, $\sqrt{s} \simeq 2m_Q$ ($Q = b, c$) this part of quark-antiquark interaction becomes important, and at large n the near-threshold region dominates in the perturbative coefficients a_n, a'_n in (141). A systematic treatment of this problem is possible in *nonrelativistic QCD (NRQCD)*, a specially designed effective theory obtained from QCD in the infinite heavy quark mass limit (for a review see, e.g. [23]).

Equally well, QCD sum rules allow to estimate the masses of light u, d, s quarks. To give only one typical example from the vast literature let me refer to the recent analysis [24], based on the correlation function for derivatives of the s-flavoured vector current $j_{s\,\mu} = \bar{s}\gamma_\mu q$, ($q = u, d$):

$$\Pi^s(q) = i \int d^4x e^{iqx} \langle 0|T\{\partial_\mu j_s^\mu(x)\partial_\nu j_s^{\dagger\nu}(0)\}|0\rangle . \tag{155}$$

The QCD answer for Π^s is proportional to $(m_s - m_q)^2 \simeq m_s^2$ (due to $\partial_\mu j_s^\mu = (m_s - m_q)\bar{s}q$), making this correlator very sensitive to m_s. One calculates the usual set of diagrams shown in Figs. 14 and 20, where the quark lines are now s and q. Furthermore, the recent progress in the multiloop QCD calculations allows to reach the $O(\alpha_s^3)$ accuracy in the perturbative part of Π^s and to include also $O(\alpha_s)$ corrections to the condensate contributions. The hadronic spectral density $\rho_K(s)$ for this correlator is saturated by $J^P = 0^+$ states with s-flavour, e.g. $K\pi$ states with $L = 0$. The sum rule has the form

$$\int ds \rho_K(s) e^{-s/M^2} = (m_s - m_{u,d})^2 \left[\Pi^{pert}(M) + \frac{C_4^K}{M^4} + \frac{C_6^K}{M^6} \right] , \tag{156}$$

Data of kaon S-wave scattering on π, η, η' were used to reproduce $\rho^K(s)$. The resulting prediction [24] for the mass is

$$m_s(2 \text{ GeV}) = 99 \pm 16 \text{ MeV}. \tag{157}$$

The ratios of the light (u, d, s) quark masses can be predicted in QCD from the relations for pions and kaons, similar to (135). A systematic derivation is done employing *chiral perturbation theory*, an effective theory obtained from QCD in the a low-energy limit, using instead of quarks and gluons, the pion and kaon degrees of freedom (for a review see [25]). The result is [26]:

$$\frac{m_u}{m_d} = 0.553 \pm 0.043, \quad \frac{m_s}{m_d} = 18.9 \pm 0.8, \quad \frac{2m_s}{m_u + m_d} = 24.4 \pm 1.5 . \tag{158}$$

From the above ratios and the value (157) one obtains $m_u(2 \text{ GeV}) = 2.9 \pm 0.6$ MeV and $m_d(2 \text{ GeV}) = 5.2 \pm 0.9$ MeV.

We see that QCD sum rules are extremely useful for the quark mass determination. The m_q values extracted from sum rules are included, together with the lattice determinations and results of other methods, in the world-average intervals in [4] presented in (31).

5.5 Calculation of the B meson decay constant

In B-meson decays the CKM parameters of the Standard Model are inseparable from hadronic matrix elements. Hence, without QCD calculation of these matrix elements with an estimated accuracy, it is impossible to use experimental data on B decays for extracting the Standard Model parameters and for detecting/constraining new physics effects. Currently, lattice QCD provides many hadronic parameters for B physics, with a continuously improving accuracy. QCD sum rules represent another actively used working tool. With condensates and quark masses determined from a set of experimentally proven sum rules for light-quark and heavy quarkonium systems, one has a real possibility to assess the theoretical accuracy of the sum rule predictions by varying the input within allowed intervals.

One of the most important applications of QCD sum rules is the determination of the B-meson decay constant f_B defined via the matrix element

$$m_b \langle 0 \mid \bar{q} i \gamma_5 b \mid B \rangle = m_B^2 f_B , \tag{159}$$

$(q = u, d, s)$. Note that f_B multiplied by V_{ub} determines the width of leptonic B decays, such as $B^- \to \tau^- \bar{\nu}_\tau$. To calculate f_B from QCD sum rules, one usually employs the correlation function:

$$\Pi_5^{(B)}(q) = i \int d^4x e^{iqx} \langle 0|T\{m_b \bar{q}(x) i \gamma_5 b(x), m_b \bar{b}(0) i \gamma_5 q(0)\}|0\rangle , \tag{160}$$

so that the lowest B meson term in the hadronic sum for this correlation function contains f_B:

$$\Pi_5^{(B)}(q) = \frac{m_B^4 f_B^2}{m_B^2 - q^2} + ... \tag{161}$$

To obtain the sum rule, one needs to calculate $\Pi_5^{(B)}(q)$ from the perturbative and condensate diagrams in Figs. 14 and 20, with γ_5 vertices emitting and absorbing b and q lines. One, therefore needs an input value for m_b and m_s ($m_{u,d}$ can safely be neglected). These values are taken from the analyses overviewed in the previous subsection. The sum rule has a form similar to (148) for f_ρ, Naturally, the expressions for the perturbative part and for the coefficients C_d are completely different. Also the hierarchy of contributions in the heavy-light correlation function differs from the light-quark case. Now the quark condensate becomes very important being proportional to $m_b\langle\bar{q}q\rangle$. The recent updates of the sum rule for f_B obtained in [27, 28] take into account the $O(\alpha_s^2)$ corrections to the heavy-light loop calculated in [29]. The numerical prediction of the sum rule, taking $m_b(m_b) = 4.21 \pm 0.05$ GeV, is: $f_B = 210 \pm 19$ MeV and $f_{B_s} = 244 \pm 21$ MeV [27], in a good agreement with the most recent lattice QCD determinations.

5.6 Light-cone sum rules and $B \to \pi$ form factor

To complete our brief survey of QCD sum rules, let me introduce one important version of this method, the light-cone sum rules (LCSR) [30, 31] used to calculate various hadronic amplitudes relevant for exclusive processes. In the following, we consider the application of LCSR to the $B \to \pi$ transition amplitude (see Fig. 9). The latter is determined by the hadronic matrix element

$$< \pi^+(p)|\bar{u}\gamma_\mu b|B(p+q) > = 2f_{B\pi}^+(q^2)p_\mu + \left[f_{B\pi}^+(q^2) + f_{B\pi}^-(q^2)\right]q_\mu, \tag{162}$$

generated by the $b \to u$ weak current (67). Due to spin-parity conservation only the vector part of the current contributes. There are two independent 4-momenta p and q, and one independent invariant q^2, the momentum transfer squared. The initial and final mesons are on shell, $p^2 = m_\pi^2$ and $(p+q)^2 = m_B^2$. It is quite obvious that one needs two invariant functions of q^2, the *form factors* $f_{B\pi}^+(q^2)$ and $f_{B\pi}^-(q^2)$, to parameterize this matrix element. Only one form factor $f_{B\pi}^+$ is interesting, the other one is kinematically suppressed in the measurable $B \to \pi l\nu_l$ semileptonic decay rate ($l = e, \mu$).

To derive LCSR for $f_{B\pi}^+(q^2)$ one uses a specific correlation function, which itself represents a hadronic matrix element. It is constructed from the product of the weak $\bar{u}\gamma_\mu b$ current and the current $m_b\bar{b}i\gamma_5 d$ used to generate B in (159). The currents are taken at two different 4-points and sandwiched between vacuum and the one-pion state. The formal definition of this correlation function reads:

$$F_\mu(q,p) = i\int d^4x e^{iqx}\langle\pi^+(p) \mid T\{\bar{u}(x)\gamma_\mu b(x), m_b\bar{b}(0)i\gamma_5 d(0)\} \mid 0\rangle$$
$$= F(q^2, (p+q)^2)p_\mu + \tilde{F}(q^2, (p+q)^2)q_\mu , \tag{163}$$

where it is sufficient to consider only one invariant amplitude F. Note that we now have two kinematical invariants, q^2 and $(p+q)^2$, still $p^2 = m_\pi^2$.

Diagrammatically, the correlation function (163) is represented in Fig. 24. At spacelike $(p+q)^2 < 0$ and $q^2 < 0$, very similar diagrams describe the process $\gamma^*\gamma^* \to \pi^0$, the one-pion production by two virtual photons via e.m. currents [14]. One only has to replace all quarks in the diagrams in Fig. 24 by either u or d quarks. Both objects: the heavy-light correlation function (163) and the $\gamma^*\gamma^* \to \pi^0$ amplitude contain one virtual quark propagating between vertices and a quark-antiquark pair which is emitted at points x and 0 and converted into a real pion state. At large spacelike external momenta $|(p+q)^2|, |q^2| \gg \Lambda_{QCD}^2$ the space-time interval $x^2 \simeq 0$ approaches the light-cone. Hence, the virtual quark in both $\langle$two-currents $\to$ pion$\rangle$ amplitudes propagates at short distances allowing a perturbative QCD description. The calculable short-distance parts are process-dependent. In case of the correlation function (163) we have a virtual b quark propagating between vertices of flavour-changing currents, whereas in the $\gamma^*\gamma^* \to \pi^0$ amplitude the light quark propagates between e.m. vertices. The long-distance part in both cases is, however, the same vacuum-to-pion matrix element of light quark and

[14]This process is experimentally accessible in $e^+e^- \to e^+e^-\pi^0$ two-photon (double-tagged) collisions.
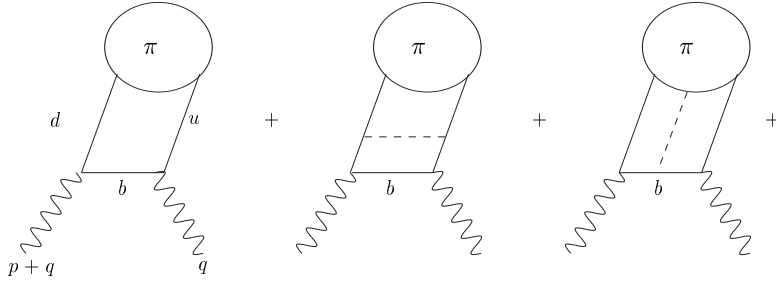
Fig. 24: *Diagrams contributing to the correlation function (163), from left to right: the leading-order, $O(\alpha_s)$ correction, soft gluon. The blob with π denotes the pion distribution amplitude.*

antiquark emitted at points x and 0:

$$\langle \pi(p) \mid \bar{q}_1(x)\Gamma_a q_2(0) \mid 0 \rangle , \tag{164}$$

where in one case $q_1 = u$, $q_2 = d$, $\pi = \pi^+$ and in the other case $q_1 = u(d)$, $q_2 = u(d)$, $\pi = \pi^0$. Due to isospin symmetry, the difference between these two configurations is indeed very small. In order to treat the diagram with one extra gluon entering the pion, one has to introduce an additional quark-antiquark-gluon matrix elements of the type

$$\langle \pi(p) \mid \bar{u}(x)g_s G^{\mu\nu}(y)\Gamma_b d(0) \mid 0 \rangle , \tag{165}$$

where $x^2 \sim y^2 \sim (x-y)^2 \to 0$. In the above $\Gamma_{a,b}$ denote certain combinations of Dirac matrices.

Having separated short- and long-distances, one is able to calculate the correlation function (163) in a form of *light-cone OPE*, where the short-distance part (the virtual b quark propagator plus gluon corrections) is multiplied by a long-distance part, the universal matrix elements such as (164), (165). The latter can be parameterized in terms of *light-cone distribution amplitudes* of the pion [32], The most important of them is defined by

$$\langle \pi(p)|\bar{u}(x)\gamma_\mu\gamma_5 d(0)|0\rangle = -ip_\mu f_\pi \int_0^1 du \, e^{iupx}\varphi_\pi(u,\mu), \tag{166}$$

where μ is a characteristic momentum scale, determined by the average x^2 in the correlation function. In the above definition, u and $1-u$ are the fractions of the pion momentum p carried by the quark and antiquark, in the approximation where one neglects the transverse momenta of the constituents with respect to the longitudinal momenta. The leading-order answer for F obtained from the first diagram in Fig. 24 using (166) is quite simple:

$$F(q^2, (p+q)^2) = m_b f_\pi \int_0^1 \frac{du \, \varphi_\pi(u,\mu)}{m_b^2 - (q+up)^2} . \tag{167}$$

The pion DA $\varphi_\pi(u)$ plays here the same role of nonperturbative input as the condensates in the conventional QCD sum rules considered above. Asymptotically, that is at $\mu \to \infty$, QCD perturbation theory implies $\varphi_\pi(u,\infty) = 6u(1-u)$. However, at the physical scale $\mu \sim m_b$, at which the OPE is applied to the correlation function (163), nonasymptotic effects also contribute, which we will not discuss for brevity. Importantly, there is a power hierarchy of different contributions stemming from the diagrams in Fig. 24, determined by the large scale in the correlation function. This scale is given by the
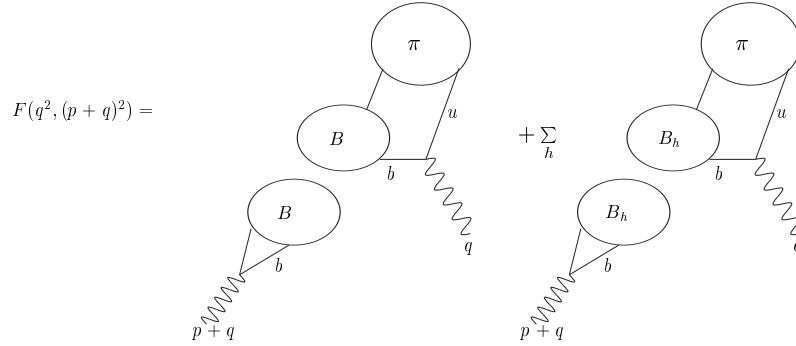
$$F(q^2, (p+q)^2) =$$

Fig. 25: *Diagramatic representation of the dispersion relation for the correlation function (163.)*

virtuality of b quark, i.e. by the quantity which stands in the denominator of the b-quark propagator: $m_b^2 - (q+up)^2 = m_b^2 - (p+q)^2 u - q^2(1-u)$. Importantly, this quantity remains large when q^2 is positive (timelike) but not very large, $q^2 \ll m_b^2$, allowing one to penetrate into the lower part of the kinematical region $0 < q^2 < (m_B - m_\pi)^2$ of $B \to \pi l \nu_l$ decay. An example of a subleading contribution is the diagram with an additional gluon entering pion DA (the third one in Fig. 24). It has two powers of inverse scale and is suppressed with respect to the leading-order diagram. Over recent years $O(\alpha_s)$ corrections and quark-antiquark-gluon contributions have been calculated to improve the result (167).

Having evaluated F as a function of q^2 and $(p+q)^2$, we are still half-way from the final sum rule. The next important step is writing down a dispersion relation in the variable $(p+q)^2$, the external momentum of the current with B meson quantum numbers. The diagrammatical representation of the dispersion relation is shown in Fig.25. It contains the same set of hadronic states as in the sum rule for f_B, starting from B meson ground state. Using (159) and (162) one obtains the hadronic representation we need:

$$F(q^2, (p+q)^2) = \frac{2 m_B^2 f_B f_{B\pi}^+(p^2)}{m_b(m_B^2 - (p+q)^2)} + \dots . \tag{168}$$

The ellipses in the above denote the contributions from the excited B and from continuum states. Equating the QCD result (167) in the region of validity $(p+q)^2 < 0$ with the dispersion relation (168) one obtains a raw sum rule relation for $f_B f_B^+(p^2)$. The rest of the calculation follows the usual QCD sum rule procedure: Borel transformation in $(p+q)^2$ and subtraction of the contribution from higher states invoking quark-hadron duality. One finally arrives at an expression for the desired form factor, the dominant term of which obtained directly from (167) is given by

$$f_{B\pi}^+(q^2) = \frac{f_\pi m_b^2}{2 f_B m_B^2} \int_\Delta^1 \frac{du}{u} (\varphi_\pi(u, \mu_b) + \dots) exp\left(\frac{m_B^2}{M^2} - \frac{m_b^2 - q^2(1-u)}{uM^2} \right) . \tag{169}$$

Here, M is the Borel mass parameter, and the scale μ_b reflects the characteristic virtuality of the correlation function, $\mu_b^2 = m_B^2 - m_b^2$. The integration limit $\Delta = (m_b^2 - p^2)/(s_0 - p^2)$ depends on the effective threshold s_0^B above which the contribution from higher states to the dispersion relation (168) is canceled against the corresponding piece in the QCD representation (167). The parameters f_B, s_0^B are usually taken from the sum rule for f_B considered in the previous subsection. The most recent predictions for $f_{B\pi}^+(q^2)$ obtained from LCSR [33] were used to extract $|V_{ub}|$ from the measurements of the exclusive

semileptonic width at B factories [34], using the formula for the decay rate:

$$\frac{d\Gamma(B \to \pi l \bar{\nu})}{dq^2} = \frac{G^2 |V_{ub}|^2}{24\pi^3} (E_\pi^2 - m_\pi^2)^{3/2} [f_{B\pi}^+(q^2)]^2 \,. \tag{170}$$

where E_π is the pion energy in the B meson rest frame.

6. CONCLUSIONS

QCD has a thirty-years history and embraces many approaches, some of them developed quite independently from the others. Due to self-interactions of gluons this theory has an extremely rich dynamics, combining asymptotic freedom at short distances with the self-emerging energy scale Λ_{QCD} and confinement at long distances. Accordingly, QCD has two different phases: the perturbative one responsible for quark-gluon processes at large momentum transfers and the nonperturbative one where the only observable states are hadrons formed by confined quarks and gluons. Yet there is no complete analytical solution for the hadronic phase of QCD. One has to rely on approximations: either numerical (QCD on the lattice) or analytical (QCD sum rules). In addition, several effective theories corresponding to different limits of QCD and exploiting the rich symmetry pattern of the theory are successfully used. In the overview of QCD given in these lectures I tried to emphasize the importance of the hadronic aspects of QCD, where the most nontrivial phenomena and challenging problems are accumulated.

References

[1] I. Aitchison, Lectures at this school.

[2] Kostandin Erznkazi, The Book of Morning Light (in Armenian), Editions "S.Grokh" 1961, Yerevan

[3] DELPHI Collaboration, events on the Z peak displayed at http://delphiwww.cern.ch/ delfigs/events/z0ps/z0maxen.html.

[4] K. Hagiwara *et al.* [Particle Data Group Collaboration], Phys. Rev. D **66** (2002) 010001.

[5] S. R. Sharpe, Lectures given at TASI 94: CP Violation and the limits of the Standard Model, Boulder, CO, hep-ph/9412243;
A. S. Kronfeld, In Shifman, M. (ed.): At the frontier of particle physics. Vol. 4, 2411-2477,hep-lat/0205021.

[6] R. Fleischer, Lectures at this School.

[7] L. B. Okun, Weak Interactions of Elementary Particles, Pergamon Press 1963.

[8] M. A. Shifman, In Boulder TASI 95:409-514, hep-ph/9510377.

[9] T. Mannel, hep-ph/9611411.
A. F. Falk, hep-ph/9812217.

[10] T. Nakano *et al.* [LEPS Collaboration], Phys. Rev. Lett. **91** (2003) 012002, hep-ex/0301020;
S. Stepanyan *et al.* [CLAS Collaboration], Phys. Rev. Lett. **91** (2003) 252001, hep-ex/0307018
V. V. Barmin *et al.* [DIANA Collaboration], Phys. Atom. Nucl. **66** (2003) 1715, hep-ex/0304040.

[11] T. Sjostrand, L. Lonnblad, S. Mrenna and P. Skands, hep-ph/0308153.

[12] A. Pich, hep-ph/0001118.

[13] G.Altarelli, Lectures given at 2001 European School of High-Energy Physics, Beatenberg, Switzerland, e-Print Archive: hep-ph/0204179.

[14] D. Diakonov, Prog. Part. Nucl. Phys. **51** (2003) 173, :hep-ph/0212026.

[15] P. Colangelo and A. Khodjamirian, In Shifman, M. (ed.): At the frontier of particle physics/Handbook of QCD, vol. 3, 1495-1576; hep-ph/0010175.

[16] V. A. Novikov, L. B. Okun, M. A. Shifman, A. I. Vainshtein, M. B. Voloshin and V. I. Zakharov, Phys. Rev. Lett. **38** (1977) 626 [Erratum-ibid. **38** (1977) 791]; Phys. Rept. **41** (1978) 1.

[17] M. A. Shifman, A. I. Vainshtein and V. I. Zakharov, *Nucl. Phys.* B **147**, 385, 448 (1979).

[18] M. Shifman, *Prog. Theor. Phys. Suppl.* **131**, 1 (1998);hep-ph/9802214;
E. de Rafael, Lectures at Les Houches Summer School, Session 68, Les Houches, France (1997), hep-ph/9802448.

[19] B. L. Ioffe, Nucl. Phys. B **188** (1981) 317 [Erratum-ibid. B **191** (1981) 591]; Z. Phys. C **18** (1983) 67.

[20] Y. Chung, H. G. Dosch, M. Kremer and D. Schall, Phys. Lett. B **102** (1981) 175; Nucl. Phys. B **197** (1982) 55.

[21] J. H. Kuhn and M. Steinhauser, Nucl. Phys. B **619** (2001) 588.

[22] B. L. Ioffe and K. N. Zyablyuk, hep-ph/0207183.

[23] A. H. Hoang, In Shifman, M. (ed.): At the frontier of particle physics. Vol. 4, 2215-2331. hep-ph/0204299.

[24] M. Jamin, J. A. Oller and A. Pich, Eur. Phys. J. C **24** (2002) 237.

[25] H. Leutwyler, Lectures given at 14th Summer School on Understanding the Structure of Hadrons (HADRONS 01), Prague, Czech Republic, 9-13 Jul 2001; hep-ph/0212325.

[26] H. Leutwyler, Phys. Lett. B **378** (1996) 313.

[27] M. Jamin and B. O. Lange, Phys. Rev. D **65** (2002) 056005.

[28] A. A. Penin and M. Steinhauser, Phys. Rev. D **65** (2002) 054006.

[29] K. G. Chetyrkin and M. Steinhauser, Eur. Phys. J. C **21** (2001) 319.

[30] I. I. Balitsky, V. M. Braun and A. V. Kolesnichenko, Nucl. Phys. **B312** (1989) 509;
V. M. Braun and I. E. Filyanov, Z. Phys. **C44** (1989) 157.

[31] V. L. Chernyak and I. R. Zhitnitsky, Nucl. Phys. **B345** (1990) 137.

[32] G. P. Lepage and S. J. Brodsky, Phys. Lett. **87B** (1979) 359; Phys. Rev. **D22** (1980) 2157;
      A. V. Efremov and A. V. Radyushkin, Phys. Lett. **B94** (1980) 245; Theor. Math. Phys. **42** (1980) 97;
      V. L. Chernyak and A. R. Zhitnitsky, JETP Lett. **25** (1977) 510; Sov. J. Nucl. Phys. **31** (1980) 544;

[33] A. Khodjamirian, R. Ruckl, S. Weinzierl, C. W. Winhart and O. Yakovlev, Phys. Rev. **D62** (2000) 114002;
      P. Ball and R. Zwicky, JHEP **0110** (2001) 019.

[34] S. B. Athar *et al.* [CLEO Collaboration], Phys. Rev. D **68** (2003) 072003.